Radiation-induced synthesis of mono- and multi-metallic clusters and nanocolloids†

Jacqueline Belloni,* Mehran Mostafavi, Hynd Remita, Jean-Louis Marignier and Marie-Odile Delcourt

Laboratoire de Physico-Chimie des Rayonnements (CNRS URA 75), Université de Paris-Sud, 91405 Orsay, France

This review is devoted to metal cluster synthesis in solution *via* radiolytic reduction of ionic precursors under the proper conditions. The size and structure of the final particles are described in relation to the nucleation and growth mechanism of the process with a special interest in oligomers and nanometric-sized particles. The influence of either a polymeric surfactant or a ligand or a support is described. The role of a chemical electron donor in the development of cluster size is explained. Particular attention is paid to the formation of bimetallic clusters and to the synthesis conditions required to obtain either a core-shell or an alloyed structure in relation to a possible intermetal electron transfer.

In chemistry it has long been known that unusual phenomena are observed whenever ultradivided matter, instead of bulk crystals, is involved in a process. In 1973, the metal arising from the reduction of monovalent copper ions by irradiation of a solution in liquid ammonia could not be found and instead additional molecular hydrogen was detected.[1] These results, compared to other previous data, for example on silver reduction in water,[2] were explained[1] by assigning to the 'quasi-atomic state' of the nascent metal specific thermodynamical properties distinct from those of the bulk metal. Therefore, this new concept implies that, as soon as formed, atoms and small aggregates of a metal, even those known as noble in the bulk state, may be corroded by the solvent with simultaneous hydrogen evolution. Experiments on the photoionization of silver atoms in solution also have shown that their ionization potential was much lower than that of the metal.[3] Indeed, through a thermodynamical cycle, the redox potential of isolated silver atoms in water was determined to be 2.6 V less than the bulk electrode potential.[4] The size-dependent redox potentials of silver clusters were progressively determined to increase with cluster nuclearity[5–9] (in contrast with the ionization potentials of bare clusters in the gas phase, which decrease with nuclearity). The phenomenon is general for all metals.

The specificity of the radiation-induced reduction of metal ions into atoms is to generate radiolytic species of strongly reducing potential, more negative than that of any ion and *a fortiori* of any charged cluster. The important features of the nuclearity-dependent potential play a crucial role when clusters are built from the progressive coalescence of atoms, as in the synthesis in solution through the reduction of ionic precursors. Therefore, the final structure and size of the clusters result from the mechanism of the growth process.

Principles

Formation of clusters

Radiolytic reducing species. Usually, metal clusters are generated by chemical reduction either of ion precursors in solution by soluble agents or of ions impregnated on solids by hot hydrogen.[10] In the present review, the atoms are produced by radiation-induced reduction of the metal ion precursors in solution, in order to control as far as possible the atom coalescence in solution that gives rise to metal clusters, possibly at a support interface. Energy deposition throughout the solution ensures an initial homogeneous distribution of the radiolytic radicals formed by ionization and excitation of the solvent, which represents the most abundant species. An example is given in the case of water:[11]

$$H_2O \rightsquigarrow e_{aq}^-, H^+, H^\cdot, OH^\cdot, H_2O_2, H_2 \quad (1)$$

The solvated electrons, e_{aq}^-, and $H^\cdot$ atoms are strong reducing agents [$E^\circ(H_2O/e_{aq}^-) = -2.87$ V_{NHE} and $E^\circ(H^+/H) = -2.3$ V_{NHE}] so that in the following step they easily reduce metal ions down to the zero-valent state:

$$M^+ + e_{aq}^- \rightarrow M^\circ \quad (2)$$

$$M^+ + H^\cdot \rightarrow M^\circ + H^+ \quad (3)$$

where M^+ is the symbol for monovalent metal ions, possibly complexed by a ligand. Similarly, multivalent ions are reduced by multistep reactions, also including disproportionation of intermediate valencies. Such reduction reactions have been observed directly by pulse radiolysis for many metal ions.[12] Most of their rate constants are known and the reactions are often diffusion-controlled. In contrast, $OH^\cdot$ radicals are able to oxidize the ions or the atoms into a higher oxidation state and thus to counterbalance the reduction reactions (2) and (3). For this reason, the solution is generally added with an $OH^\cdot$ radical scavenger. Among various possible molecules, the preferred choice is for solutes whose oxidation by $OH^\cdot$ yields radicals that are unable to oxidize the metal ions but, in contrast, themselves exhibit strong reducing power, such as the radicals of secondary alcohols or of the formate anion:

$$(CH_3)_2CHOH + OH^\cdot \rightarrow (CH_3)_2\dot{C}OH + H_2O \quad (4)$$

$$HCOO^- + OH^\cdot \rightarrow COO^{\cdot -} + H_2O \quad (5)$$

$H^\cdot$ radicals are scavenged by these molecules as well:

$$(CH_3)_2CHOH + H^\cdot \rightarrow (CH_3)_2\dot{C}OH + H_2 \quad (6)$$

$$HCOO^- + H^\cdot \rightarrow COO^{\cdot -} + H_2 \quad (7)$$

The radicals $(CH_3)_2\dot{C}OH$ and $COO^{\cdot -}$ are almost as powerful reducing agents[13,14] as $H^\cdot$ atoms: $E^\circ[(CH_3)_2CO/(CH_3)_2\dot{C}OH] = -1.8$ V_{NHE} at pH 7 and $E^\circ(CO_2/COO^{\cdot -}) = -1.9$ V_{NHE}, respectively.

† Non-SI units employed: 1 eV ≈ 9.65 J mol^{-1}, 1 atm ≈ 101 kPa.

Metal cation reduction. The radicals are able to reduce metal ions:

$$M^+ + (CH_3)_2\dot{C}OH \rightarrow M^\circ + (CH_3)_2CO + H^+ \quad (8)$$

$$M^+ + COO^{\cdot -} \rightarrow M^\circ + CO_2 \quad (9)$$

The atoms are formed with a homogeneous distribution throughout the solution. The binding energy between two transition metal atoms is stronger than the atom–solvent or atom–ligand bond energy. Therefore, the atoms dimerize when they encounter or associate with an excess of ions:

$$M^\circ + M^\circ \rightarrow M_2 \quad (10)$$

$$M^\circ + M^+ \rightarrow M_2{}^+ \quad (11)$$

By a multi-step process these species progressively coalesce into clusters following homogeneous kinetics:

$$M_{m+x}^{x+} + M_{n+y}^{y+} \rightarrow M_{p+z}^{z+} \quad (12)$$

where m, n and p represent the nuclearities (*i.e.* the number of reduced atoms they contain) and x, y and z are the number of associated ions (Fig. 1). The redox potential of the clusters increases progressively with the nuclearity. The result is that the coalescence process competes from the earliest steps with spontaneous corrosion by the solvent, which may even prevent the formation of clusters,[1] as is the case of most non-noble metals. Monomeric atoms and oligomers of these elements are so fragile to reverse oxidation by the solvent and radiolytic protons that only H_2 is evolved. For this reason, in these systems it is preferable to scavenge the protons by adding a base to the solution (Fig. 1) and to favour the coalescence by a reduction faster than the oxidation, which obeys first-order kinetics.[1,15]

Cluster stabilization. Metal atoms formed by irradiation or any other method tend to coalesce into oligomers, which themselves progressively grow into larger clusters and eventually into precipitates, as found in early radiolytic experiments.[16] However, the coalescence may be limited, provided a polymeric molecule acting as a cluster stabilizer is added. Functional groups with a high affinity for the metal ensure the anchoring of the molecule at the cluster surface while the polymeric chain protects the cluster from coalescing with the next one and thus inhibits at an early stage further coalescence through electrostatic repulsion or steric hindrance. Some of these polymeric systems are, at the same time, the stabilizer and the reducing agent used to synthesize the metal clusters.[9,17] When metal clusters are to be prepared by irradiation, the stabilizing polymers must be selected for their inability to reduce the ions directly before irradiation. Poly(vinyl alcohol) (PVA),[18] sodium dodecylsulfate (SDS),[18] sodium poly(vinylsulfate) (PVS),[19] poly(acrylamide) (PAM) or poly(*N*-methylacrylamide) (PNMAM),[20] carbowax[21] and poly(ethyleneimine) (PEI)[22,23] do not reduce ions and fulfill the conditions for stabilization. The final size of metal clusters stabilized by these polymers lies in the nanometric range and the sol presents the classical surface plasmon absorption band of the metal. In contrast, sodium polyacrylate (PA) is a very strong stabilizer that allows the formation of long-lived metal oligomers.[24] It was concluded that the metal–acrylate interaction is comparable to a rather strong ligation. Polyphosphate (PP) was also found to act as a strong stabilizer, yielding small oligomers at the end of irradiation but these particles undergo further coalescence of within tens of minutes.[25]

Some ligands (*e.g.*, CN^-, EDTA) are able by themselves to stabilize small-sized particles. The coalescence of atoms into clusters may also be restricted by generating the atoms inside the confined volumes of microheterogeneous structures in porous materials or of microorganized systems.[26] The ionic precursors are included prior to irradiation. Then the clusters are trapped in the microvolumes, where they are still accessible to the reactants. The surface of solid supports adsorbing metal ions is a strong limit to the diffusion of the nascent atoms formed by irradiation at room temperature, so that quite small clusters can survive. The stabilization of radiation-induced clusters at the smallest sizes by a polymer or a support is one way to benefit from the specific properties appearing for the lowest nuclearities.[1–7]

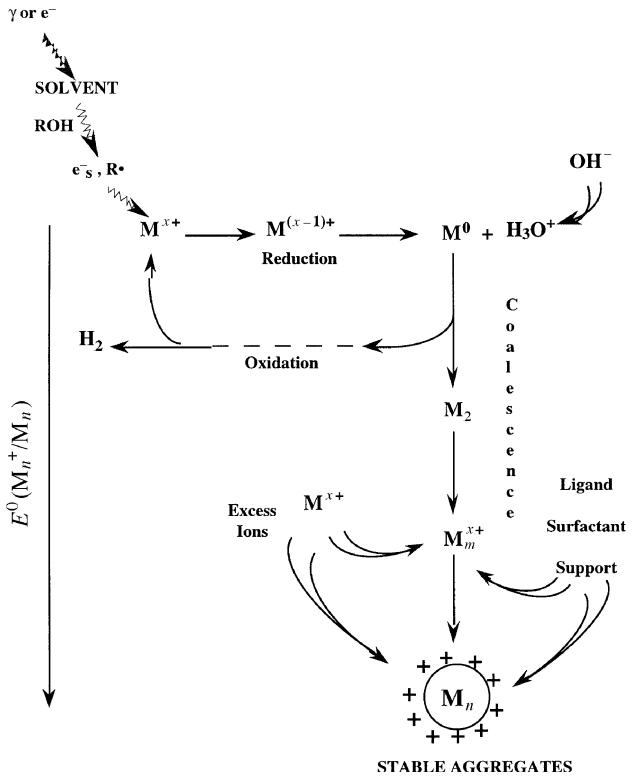

Fig. 1 Scheme of metal ion reduction in solution by ionizing radiation. The isolated atoms formed coalesce into clusters. They adsorb an excess of ions. They are stabilized by ligands, polymers or supports. The redox potential increases with the nuclearity. The smallest oligomers may undergo reverse corrosion

Synthesis features. The specificity of the radiation-induced synthesis of metal clusters is that the redox potential of the reducing agent is so negative that the free metal ions (and not only the adsorbed ones) are generally reduced at each encounter. The isolated atoms thus created coalesce and yield monodisperse-sized clusters. Likewise, as in other chemical reductions, an excess of metal ions adsorb at the surface of these clusters, where they may be reduced by radiolytic radicals. The radiation also penetrates homogeneously even into pores or at the surface of supports of multiphase systems, where the clusters are formed *in situ*. The reduction is efficient at room temperature, so that supports fragile to heat, such as polymeric systems that are not suitable for chemical reduction under heating, may be used in the irradiation process. The reduction rate is controlled by the selected dose rate, which offers a wide range of conditions from slow to quasi-instantaneous atom production. Moreover, coupling of pulse irradiation with time-resolved observation provides important information on the particle growth mechanism (identification of transients, rate constants) and its influence on the final structure of the clusters.

Techniques

Irradiation techniques. The γ-irradiation sources used were the ^{60}Co γ-facilities of 7000 Ci (our laboratory) and 9000 Ci (PAGURE, CEN Saclay) and a ^{137}Cs γ-facility of 2000 Ci (Curie Institute, Orsay). The dose rates used varied from 0.25 kGy h^{-1} to 35 kGy h^{-1} (25 krad h^{-1} to 3.5 Mrad h^{-1}).

Other irradiation experiments were performed with a 20 kW and 10 MeV electron accelerator (CARIC Society) delivering trains of 14 ms (10–350 Hz) pulses through a scanning beam (10 Hz) of mean dose rate 2.2 kGy s^{-1} (or 7.9 MGy h^{-1}). Under our conditions the total reduction is obtained within a few seconds. The dose used is at most that necessary for complete reduction. Otherwise, by still increasing the dose, the polymer could be cross-linked.

Pulse radiolysis[11,27] allows time-resolved UV to near infrared optical spectroscopy of a solution from just after a pulse (3 ns) delivered by an electron accelerator (Febetron 706, 600 keV) up to the formation of stable clusters.

Cluster characterization. As the cluster properties depend on the nuclearity principally at low n values, where observation is the most difficult (and even more so for bimetallic particles), different adapted approaches had to be used. Characterization of stable clusters has been carried out by techniques such as UV/VIS and IR absorption spectroscopies of sols for the surface interactions with the surrounding solvent and for the identification of molecular clusters, by TEM, AFM or STM imaging for size and morphology, and by ESR, NMR, EXAFS, X-ray or EDS and EDAX for the structure and composition.‡ For some multimetallic samples, efficiency in a special catalytic application is used as an indirect check of their alloyed character.

Monometallic Clusters

Stabilized metal oligomers in solution

Silver oligomers. The optical absorption spectrum of a water solution containing silver ions complexed by polyacrylate PA and partially reduced by γ-irradiation is shown in Fig. 2. After the irradiation the absorption spectrum is quite different from the well-known surface plasmon band of nanometric silver clusters centered around 400 nm.[24,28] At low doses two peaks are observed at 275 and 350 nm.[29] Pulse radiolysis experiments of the same solution allowed the assignment of the 275 nm band to the charged Ag_4^{2+} clusters.[30] Their dimerization is quite slow (about 10^5 l mol^{-1} s^{-1}) compared to hydrated clusters. The band at 350 nm results from the PA anion interaction with the cluster. At higher doses, the 350 nm band fades away, while the 275 maximum is progressively shifted to 292 nm and another band develops around 480 nm (Fig. 2). Then, this band itself is slowly shifted to the red and is eventually observed up to 800 nm (Fig. 3). The colour of the stable solution is blue. The spectrum is assigned to the product of Ag_4^{2+} dimerization containing 4 reduced silver atoms and absorbing at 292 nm.[24,25] The kinetics of the UV bandshift depends on the initial Ag_4^{2+} concentration, whereas the kinetics of the visible band shift from 480 to 800 nm is very sensitive to the polyanion concentration. The visible absorption is assigned to a cluster–ligand interaction with PA.[24]

The 'blue' silver clusters are stable for years, even in the presence of air. The exceptional stability of the clusters makes possible the study of their physical and chemical properties by a wide range of techniques.[32] In particular, these clusters have been imaged by STM after being deposited on a HOPG (highly oriented pyrolytic graphite) surface. Clear images with atomic resolution are observed (Fig. 3) showing flat clusters of 0.7 nm with atoms spaced by 0.25 nm.[33] Each cluster contains seven nuclei (possibly with an eighth atom in the central position). Since 4 atoms only were reduced ($n = 4$), they correspond to the stoichiometry Ag_7^{3+} (or Ag_8^{4+}).

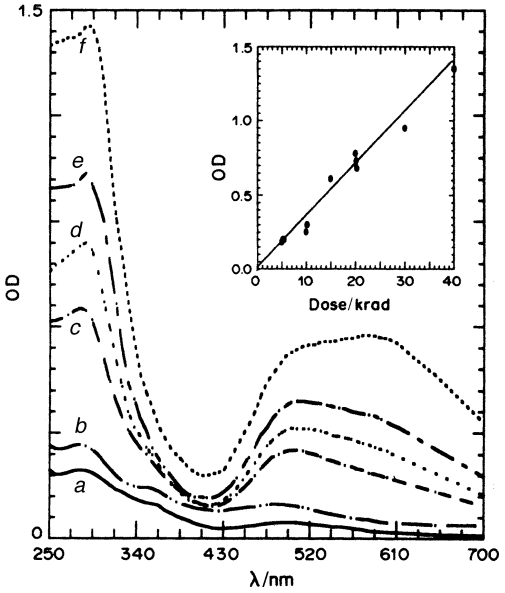

Fig. 2 Absorption spectra of a solution containing 10^{-3} mol l^{-1} Ag_2SO_4, 0.2 mol l^{-1} PA and 0.1 mol l^{-1} 2-propanol at pH 10.3, γ-irradiated at increasing dose: (*a*) 5, (*b*) 10, (*c*) 15, (*d*) 20, (*e*) 30, (*f*) 40 krad (or 0.4 kGy). Optical length $l = 5$ mm. Inset: Optical density at the maximum *vs.* dose. (Reproduced with permission from Ref. 29. Copyright 1992 Elsevier Science)

Platinum oligomers. When $PtCl_6^{4-}$ ions are irradiated, even to complete reduction in the presence of PA polymer, a few 1 nm clusters are observed, but most of the Pt atoms are found in the form of very small oligomers. Despite the absence of adsorbed Pt ions, the stabilization by PA prevents aggregation and STM imaging shows 3–7 Pt atom oligomers.[34] In the presence of PP, the irradiated solution presents a UV band with a maximum at 215 nm.[35] About 20% of the initial signal is lost by oxidation when the sample is exposed to air, the rest being stable. This result again confirms that the redox potential of the smallest clusters is markedly shifted to negative values.

Copper oligomers. In the case of $CuSO_4$ solutions irradiated with PA at pH 10, new absorption bands at 292, 350 and 455 nm are observed, provided that the reduction of copper ions is partial (Fig. 4).[36] The absorption spectra of copper oligomers are totally different from the usual plasmon band, which is obtained at around 570 nm in the presence of PVA as the stabilizer. The plasmon band develops only at high irradiation dose (Fig. 4, top) and the intensity of the peaks at shorter wavelengths decreases correlatively. A pulse radiolysis study of monovalent Cu^+ solutions complexed in the presence of a high concentration of Cl^-, but without any polymeric stabilizer, has shown that short-lived states of reduced copper corresponding to the early steps of growth also absorb in the range of 355–410 nm.[37] Moreover, the species absorbing in the UV are very sensitive to oxygen.[36] For these reasons the species absorbing in the UV are attributed to the early stages of nucleation of Cu aggregates. Note that under acidic conditions, where the PA polymer is present in its protonated form, the oligomers absorbing in the UV are not observed. Instead, the decay of Cu^+ at 480 nm is correlated with the formation of large nanoaggregates absorbing at 570 nm (Fig. 4, bottom).

Nickel oligomers. Among the non-noble metal clusters that can be synthesized by radiation-induced reduction in solution, nickel raises some difficulties since the atom formation and aggregation processes undergo the competition of oxidation reactions of highly reactive transients, such as monovalent Ni^+ion, Ni atom and the very first oligomers. Nevertheless, in

‡ Acronyms used here and later in the article are: TEM, transmission electron microscopy; AFM, atomic force microscopy; STM, scanning tunnelling microscopy; ESR, electron spin resonance; EXAFS, extended X-ray absorption fine structure; EDS, electron diffraction spectroscopy; EDAX, energy dispersive X-ray analysis; QELS, quasi elastic light scattering; RBS, Rutherford back scattering.

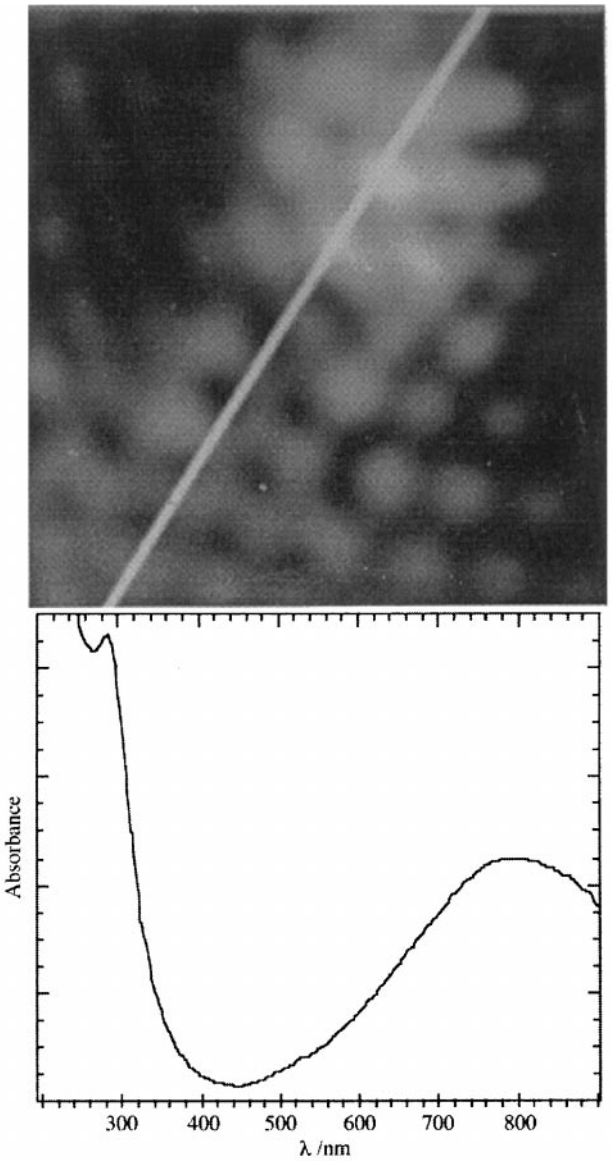

Fig. 3 Silver clusters formed in a partially reduced solution of 10^{-3} mol l^{-1} Ag_2SO_4 by γ irradiation (0.10 kGy) in the presence of PA, 75 days after irradiation. Upper: STM imaging of a single cluster of the blue sol. (Reproduced with permission from ref. 33. Copyright 1994). Lower: absorption spectrum of the blue sol. (Reproduced with permission from ref. 31. Copyright 1990)

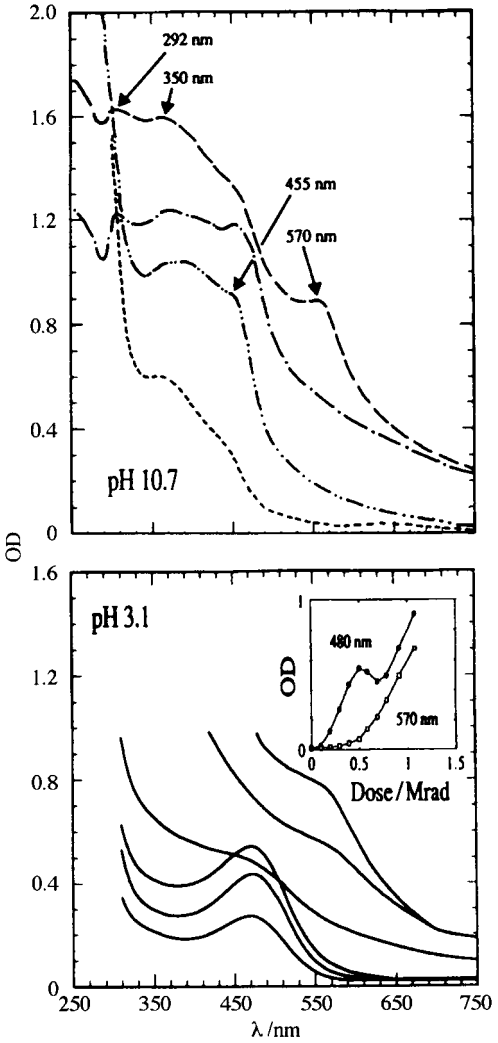

Fig. 4 Evolution with dose of the optical absorption spectrum of an irradiated Cu^{2+} solution: 10^{-3} mol l^{-1} $CuSO_4$, 0.2 mol l^{-1} 2-propanol, 0.1 mol l^{-1} PA. Top: pH = 10.7; (-----) 0.06 (··-··) 0.12, (-·-·-·-) 0.47, (–––) 1.04 Mrad. Bottom: pH 3.1 Inset: evolution with dose of the 480 and 570 absorption bands. (Reproduced with permission from ref. 36. Copyright 1992)

the presence of PA, a new absorption band develops at 540 nm with increasing dose. The formation of the same absorption band was observed by pulse radiolysis: this band increases simultaneously with the formation of the very first Ni atoms and is attributed to a cluster–ligand interaction. Due to the high reactivity of nickel oligomers, the band disappears within 24 h even when solutions are preserved from oxygen, through a spontaneous reaction with the solvent.[38]

Molecular metal clusters

When the irradiation of metal ion solutions is carried out in the presence of a ligand, such as CO[39] or PPh_3,[40] metal reduction, ligation and aggregation reactions compete, leading to reduced metal complexes and then to molecular clusters. Increasing the [metal precursor] : [ligand] ratio favors higher nuclearities. The structure depends on the metal precursor. The radiolytic reduction of metal ions under CO atmosphere (1 atm) is achieved in alcohols to increase CO solubility.

By irradiating K_2PtCl_4 under CO in a mixed equivolumic water–2-propanol solution, the Chini clusters $[Pt_3(CO)_6]_m^{2-}$[41] with $m = 3$–10 (*i.e.* 9–30 Pt atoms) have been obtained.[39,42] The m value is deduced from the very specific UV/VIS and IR absorption spectra. The reduction occurs by the radiolytic radicals and also by an additional effect of CO. The synthesis is selective and m is controlled by adjusting the dose (high doses yield low m values) (Fig. 5). Molecular clusters $[Pt_3(CO)_6]_m^{2-}$ have been observed by scanning microscopy (STM) with $m = 5$ (Fig. 6). On increasing markedly the [Pt] : [CO] ratio, other carbonyl clusters [denoted $Pt_x(CO)_y$ in the following] derived from the previous ones are obtained.[43] Fig. 5 presents the spectral evolution of such a system with increasing dose. At low doses, $[Pt_3(CO)_6]_m^{2-}$ clusters are first formed until about half of the platinum ions are reduced, then the shape corresponds to clusters containing fewer CO ligands per Pt atom. After deposition on carbon or α-alumina, the structure of these Pt clusters has been investigated by EXAFS.[44] For $[Pt_3(CO)_6]_m^{2-}$ clusters ($m = 4$–6) supported on carbon powder, only the Pt—Pt intra-triangle distance (0.266 nm) can be observed and some carbonyl ligands remain ligated to platinum. Nevertheless, when the samples are exposed to air, the 0.277 nm distance known to be that of bulk (fcc) Pt is also found, thus indicating that the previous clusters are partially tranformed into bulky fcc clusters. For the $Pt_x(CO)_y$ clusters deposited on carbon, both

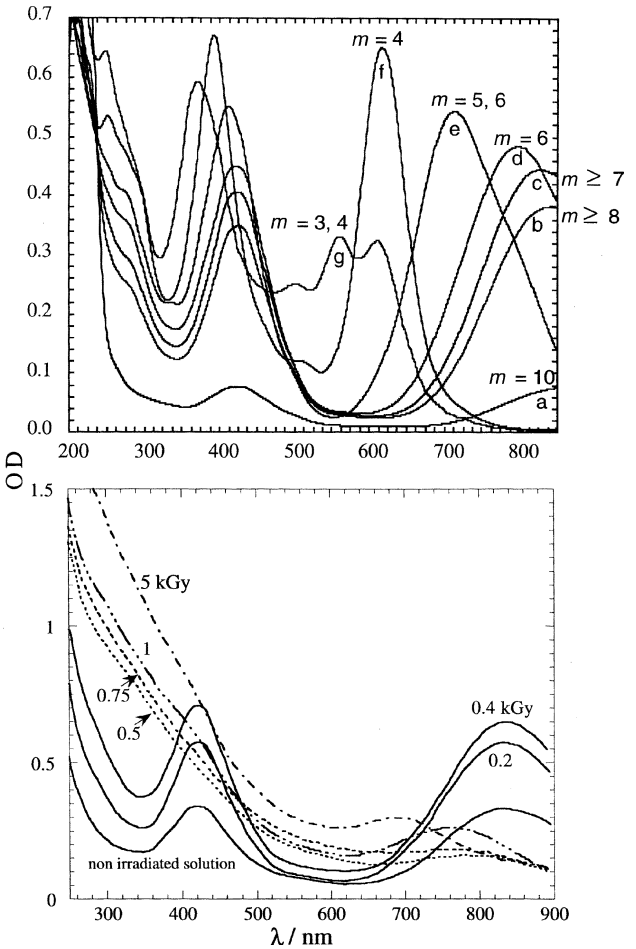

Fig. 5 UV/VIS spectra of irradiated solutions of K_2PtCl_4 in 50%/50% *v*/*v* H_2O–2-propanol under 1 atm CO with various doses. $l = 2$ mm. Top: 10^{-3} mol l^{-1} K_2PtCl_4 (*a*) before irradiation, (*b*) 0.20, (*c*) 0.40, (*d*) 0.80, (*e*) 1.60, (*f*) 3.20, (*g*) 10 kGy. Bottom: 2×10^{-3} mol l^{-1} K_2 $PtCl_4$. (Reproduced with permission from ref. 42. Copyright 1996 Elsevier Science)

0.266 nm (intra-triangle) and 0.270 nm (inter-triangle) distances are found.

Radiolysis of $RuCl_3$ under a CO atmosphere leads to the reduced valency compound $[Ru^{II}(CO)_3Cl_2]_2$, but if Cu powder as a chloride acceptor is added, a mixture of the polynuclear $Ru_3(CO)_{12}$ and $H_2Ru_6(CO)_{18}$ clusters is obtained.[39] At increasing concentration, the formation of $H_2Ru_6(CO)_{18}$ becomes preponderant over that of $Ru_3(CO)_{12}$. Then large metal aggregates are synthesized.

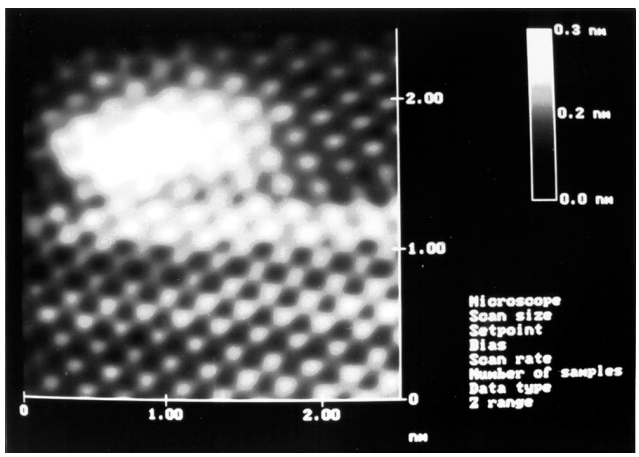

Fig. 6 STM image of a Chini cluster ($m = 5$) from a solution deposited on an HOPG graphite surface. (Reproduced with permission from ref. 43. Copyright 1996 Academic Press)

Radiolysis of $FeCl_2$ in alcoholic solutions under a CO atmosphere leads to the formation of the mononuclear cluster $Fe(CO)_5$.[39,40] The conversion is achieved with a dose around 60 kGy. The transformation ratio depends on the alcohol (25%, 35% and 70% in methanol, ethanol and isopropanol respectively). When the initial [M] : [L] ratio increases, simultaneous formation of $Fe_3(CO)_{12}$ and $Fe(CO)_5$ occurs. Similarly, $Co_2(CO)_8$ may be generated by irradiation.[45]

In the case of osmium, the radiolysis of $OsCl_3$ does not yield the zero-valent state, contrary to ruthenium, even in the presence of Cu powder. However, two osmium carbonyl clusters, $[Os_5(CO)_{15}]^{2-}$ and $[HOs_5(CO)_{15}]^-$, have been synthesized from the precursor K_2OsO_4.[45]

$Rh_6(CO)_{16}$[46] is formed by radiolysis of $RhCl_3$ under CO and in the presence of Cu powder while irradiation of $[Rh^{II}(CH_3CO_2)_2]_2$ yields $[Rh_{12}(CO)_{30}]^{2-}$.[40,47]

Some mixed bi- or tri-nuclear carbonyl clusters have been also synthesized such as $FeRu_2(CO)_{12}$, $RuOs_2(CO)_{12}$ and $Ru_2Os(CO)_{12}$.[39]

Substituted phosphines and other cumbersome ligands are known to stabilize large full-shell clusters (M_{13}, M_{55}, M_{147}, ...) with cuboctahedral or icosahedral geometries obtained by chemical synthesis.[48,49] In the presence of the ligands triphenylphosphine PPh_3 or tertiobutylphenylphosphine ([M] : [L] = 0.1 to 5) in alcohols or acetone,[40] irradiation has been shown to induce phosphine-stabilized species: osmium, ruthenium and rhodium clusters with high nuclearity (M_{55} and M_{147}) or colloids have been synthesized.

Nanometric clusters

When the interaction of a stabilizer (either a polymer or a ligand) with the clusters is not extremely strong, as in the case of PA or CO, the coalescence of atoms is stopped at larger sizes than oligomers, typically in the nanometric range. According to extensions of the Mie model,[50,51] the shape of the surface plasmon optical absorption spectrum depends on the metal and on the cluster size. For a given size of a metal cluster, experimental data also show that the shape depends to some extent on the environment (solvent,[52] adsorbed ions[9] and polymer or ligand[17,53]). Despite the maximum position and intensity dependence, this optical property makes it possible to follow the kinetics of the cluster formation by pulse techniques or of their growth at increasing doses. Table 1 presents the list of metal clusters obtained by irradiation with their optical properties.[8]

As a general rule, the higher the ratio $[M^+]$: [polymer], the larger is the final size because the polymer is less protective and also the ionic strength induced by the metal salt favors coalescence.

Noble metal clusters. The ions of these metals are easily reduced into the zero-valence state. The small clusters (and also the intermediate valences) do not reduce the solvent, so that they may be stabilized at small sizes. Various metal clusters with a wide variety of surfactants have been obtained by the radiolytic method[7,8] (Table 1).

The clusters are generally stable in air, which makes them useful in numerous applications. The nuclearity ranges from a few tens of atoms (around 1 nm diameter) for Ir_n, Pt_n, for example, to 10^2–10^4 for other noble metals such as Ag_n, Pd_n, Au_n. These small-sized clusters are most often spherical. Nevertheless, large clusters of Pd_n formed without surfactant exhibit clearly pentagonal shapes with a fcc structure, as observed by electron diffraction, which suggests the formation of twin fcc crystallites growing from the faces of an icosahedral nucleus.[54]

Phase imaging in tapping mode AFM is a powerful tool for the characterization of clusters stabilized by polymer matrices, as shown recently for the first time in observing silver and

Table 1 Radiation-induced metal clusters. Optical absorption properties

Metal	λ_{max}/nm	Ref.	Metal	λ_{max}/nm	Ref.	Metal	λ_{max}/nm	Ref.
Co	UV	54, 55	Pd	205	54–56	Ir	UV	54, 55, 57
Ni[a]	UV	54, 55 58, 59	Ag[a]	380	60, 61	Pt[a]	215	20, 35, 54, 55, 60, 63
Cu[a]	570	37, 54, 55	Cd[a]	260	64, 65	Au[a]	520	66, 67
Zn	UV	54, 55	In[a]	270	37	Hg[a]	500	37, 54, 55
Mo	UV	54, 55	Sn	UV	54, 55	Tl[a]	300	37, 68–70
Ru	UV	54, 55	Sb	UV	52, 55	Pb[a]	220	37, 53, 54, 71, 72
Rh	UV	54, 55	Os	UV	53, 54	Bi	253	37, 54, 55, 73

[a] The earliest steps of the cluster formation have been studied by pulse radiolysis.

gold samples.[74] The phase detection brings a substantial improvement in the contrast for nanoscale features and helps to discriminate between amorphous polymer and metal clusters, as shown in Fig. 7 for silver nanoclusters (PA) after total reduction.

Non-noble metal clusters. Nickel or cobalt are examples of non-noble metals whose monomers and oligomers are quite fragile to corrosion by the solvent, up to nuclearities larger than for noble metals. Therefore, the production of small particles results from a compromise between the smallest size and the highest stability. It has been shown that in aqueous solutions, for example of Ni^{2+},[54,55,58,59] Co^{2+},[54,55] Sn^{2+} [54,55,75] or Tl^{+},[37,68–70] provided they are irradiated in basic medium and in the presence of $OH^{\cdot}$ radical scavengers, long-lived clusters are formed. (In order to avoid precipitation of the metal hydroxide by the base, the polymer is added first.) Their size depends on the nature of the surfactant added to the solution. Nickel clusters formed in the presence of PVA have a mean diameter of about 20 nm (Fig. 8).[57] They display ferromagnetic behavior but due to their small size, their separation from the solvent in a 1 T magnetic field takes several days. Since PA is known to stabilize small oligomers, we used a mixture of the polymers PA and PAM (polyacrylamide) in order to secure the stabilization of the very first atoms by PA while PAM acts as a stabilizing surfactant for larger clusters that could not be stabilized by PA. In the presence of both polymers, it has been possible to stabilize nanometric clusters of 4 nm in diameter.[38] The size distribution of Pb clusters (PVA) is bimodal with peaks around 2 and 15 nm.[54] Although long-lived in the absence of air, Ni or Co clusters as well as Pb clusters are readily oxidized in air. Zn clusters are formed also in basic solutions but they are reversely oxidized by the medium into zinc hydroxide within a few weeks in the absence of air.

Developed clusters

The specificity of this method is to combine the ion reduction successively: (*i*) by irradiation reduction: indeed, homogeneous formation of atoms generally requires strong reducing agents (radiolytic radicals). Then the atoms independently formed in the bulk coalesce into oligomers [reactions (1)–(12)] and (*ii*) by chemical reduction: beyond a certain oligomer nuclearity, for which the redox potential allows electron transfer from a conventional donor D, this chemical agent achieves the reduction of the rest of the ions after they have been adsorbed on the radiation-induced clusters acting as nuclei for catalytic reduction and growth. The redox threshold fixed by the donor imposes a critical nuclearity n_c for the growth process.

$$M^{+} + M_{n_c} \rightarrow M_{n_c+1}{}^{+} \quad (13)$$

$$M_{n_c+1}{}^{+} + D \rightarrow M_{n_c+1} + D^{+} \quad (14)$$

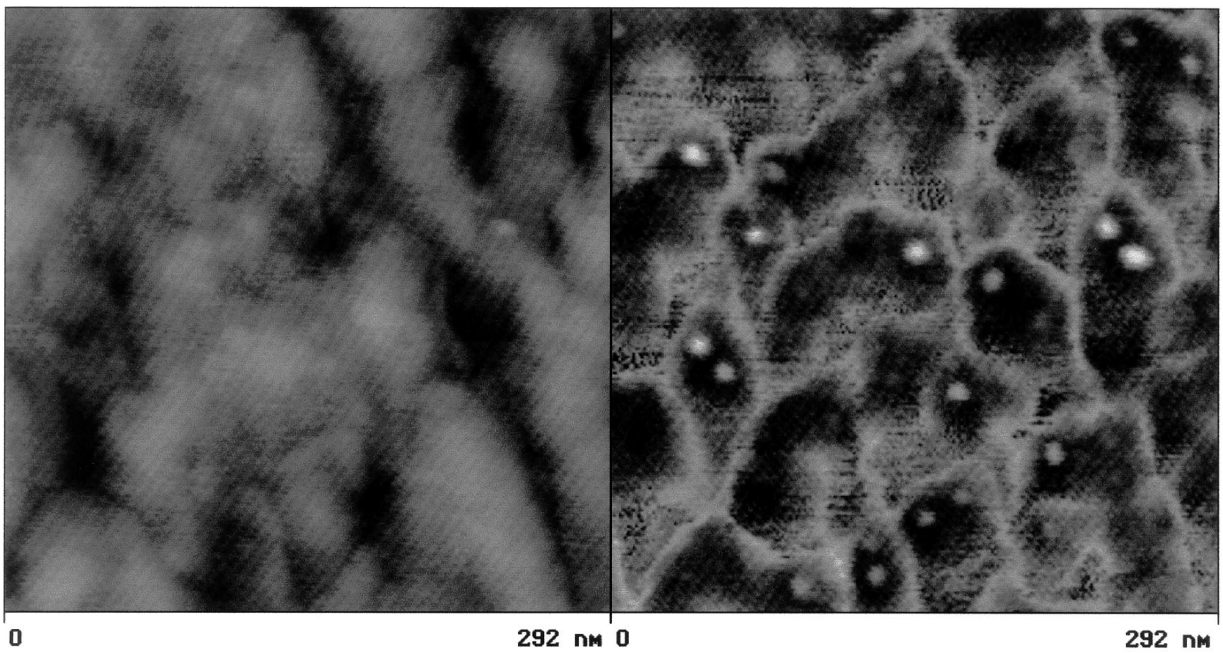

Fig. 7 AFM images of silver clusters prepared by radiolysis (electron accelerator) of a solution containing Ag_2SO_4 (10^{-3} mol l^{-1} Ag^{+}), 10^{-1} mol l^{-1} PA and 2×10^{-2} mol l^{-1} 2-propanol, dose of 3 kGy. Deposited on mica. Left: high mode. Right: phase mode. Scan size: 292 nm, setpoint: 2.749 V, scan rate: 1.001 Hz, number of samples: 512. (Reproduced with permission from ref. 74. Copyright 1997 Gauthier–Villars and CNRS)

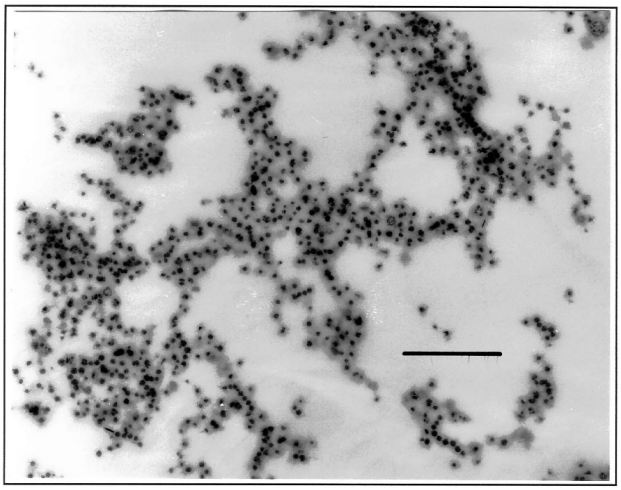

Fig. 8 Low magnification TEM bright-field image of 20 nm Ni clusters. Dose rate: 3.2 kGy h^{-1}. $[Ni^{2+}] = 2 \times 10^{-3}$ mol l^{-1}, [2-propanol] = [PVA] = 0.2 mol l^{-1}. Scale bar: 500 nm. (Reproduced with permission from ref. 58. Copyright 1985)

$$M^+ + M_{n_c+1} \rightarrow M_{n_c+2}{}^+ \quad (15)$$

$$M_{n_c+2}{}^+ + D \rightarrow M_{n_c+2} + D^+ \quad (16)$$

A moderate chemical reducing agent is unable directly to reduce free ions and ions adsorbed on subcritical clusters. This mechanism has been thoroughly studied by pulse radiolysis in the case of silver[5] and copper[76] and presents the same features as the photographic development process. Adjusting the respective amounts of ions radiolytically and chemically reduced allows us to control the cluster concentration (equal to that of the nuclei) and their final size after development with an excellent homodispersity. In photography the amplification factor is typically 10^8.[77]

By contrast, in the absence of preformed nuclei, a chemical reduction with a moderate reducing agent may occur indeed exclusively at the surface of cell walls and pre-existing dust particles where the adsorbed ions can exhibit the suitable redox potential higher than that of the donor. Consequently the mean size of the population of final clusters would be rather large and quite heterodisperse due to the non-controlled development.

Note also that for multivalent precursors the very negative potential between the transient monovalent M^+ and free atoms M^0 often inhibits the disproportionation of 2 M^+ into M^{2+} and M^0 (see examples below). However, when clusters are already formed the disproportionation may occur at their surface because the potential of the couple $M_n, M^+/M_{n+1}$ is shifted to much higher values. This process, which needs to be catalyzed by the clusters, also contributes to their development; nevertheless, the early nuclei must have been generated from free ions by a strong reducing agent.

Metal particles–organic radicals. The development mechanism [reactions(13)–(15)] has been established through pulse radiolysis by using electron donors formed within the same pulse as the silver atoms. These organic radicals, which are the reduced form of viologens (sulfonatopropyl-, $SPV^{-\cdot}$ or methylviologen, $MV^{+\cdot}$) or of naphtazarin, are followed by the intense absorbance change consecutive to the electron transfer towards supercritical silver clusters as in reactions (14) and (16).[5,6] For example, the critical size has been found to be $n_c = 4$ for $SPV^{-\cdot}$ and 85 for naphtazarin semiquinone at pH 4.8. The fraction of metal ions directly reduced by the radiolytic species into atoms start coalescing, while the reducing organic radicals are ready to play their role of electron donor soon after the pulse. Along with increasing nuclearity, the cluster redox potential increases, but as long as it is not higher than that of the donor, the coalescence kinetics are the same as in the absence of donor [reactions (1)–(12)]. Beyond the threshold fixed by the donor potential, the critical clusters accept electrons from D [reaction (14)] and after adsorption of an additional ion [reaction (15)] they repeatedly accept another electron [reaction (16)], acting as growth nuclei for a catalytic process of accumulation of all the metal atoms chemically reduced. Thus, their concentration is constant but they are developed in size. The final cluster diameter increases, for example for silver, from 15 nm (without developer) to 50 nm at the higher ratio between the concentrations of atoms chemically reduced by the donor and radiolytic nuclei (note that no polymer is added). Correlatively, a red shift is observed in the final optical surface plasmon band (Fig. 9).[5]

The time-resolved observation of the donor absorbance decay also provides the means to determine the critical nuclearity fixed by a given donor. The existence of an induction time in the donor decay directly confirms that, below the critical nuclearity, isolated ions, or ions adsorbed onto too small oligomers, are unable to be reduced by the donor and that the catalytic reduction is indeed controlled by the nuclei generated by the strongly reducing radiolytic species.

Similar experiments carried out on silver ions complexed by CN^- (donor $MV^{+\cdot}$) show that the redox potential of these clusters is lower than with the sulfate counter ion.[78] Even large clusters complexed with CN^- are easily oxidized by oxygen. In the case of gold in the presence of CN^- ligands, the smallest oligomers are readily oxidized by MV^{2+} and even disappear before coalescing.[79] With copper clusters, the redox potential also increases with the nuclearity and is more negative than for silver at equal n values.[76]

Silver particles–EDTA. Note that the non-irradiated solution of EDTA silver complex is stable and thus that EDTA does not reduce the ions. The spectra of an irradiated solution, only partially reduced, display a single band at 400 nm due to nanosized silver clusters and do not show any absorption in the red part of the spectrum (Fig. 10).[53] Then, as a post-effect, the band intensity increases with time without shifting to longer wavelengths [Fig. 10(*b*)]. The maximum of the absorbance at 400 nm is reached several days later. According to the value of the extinction coefficient, the silver ions are almost totally reduced. The post-irradiation

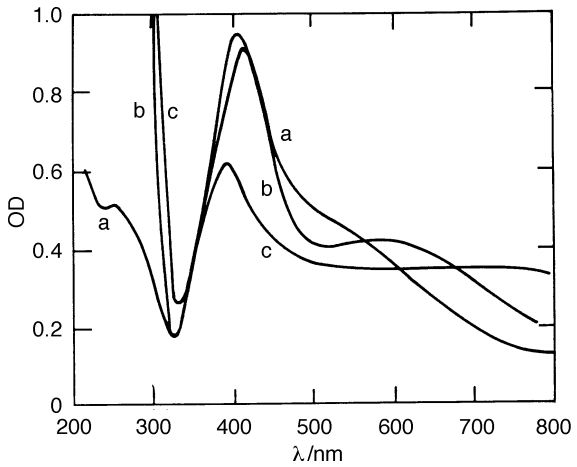

Fig. 9 Spectra of Ag_n after γ irradiation (dose 40 krad) of a solution containing $[Ag^+] = 10^{-4}$ mol l^{-1}, [2-propanol] = 0.2 mol l^{-1}. (*a*) Without SPV, (*b*) with 10^{-4} mol l^{-1} SPV, (*c*) with 10^{-2} mol l^{-1} SPV. (Reproduced with permission from ref. 5(*a*). Copyright 1989 Elsevier Science)

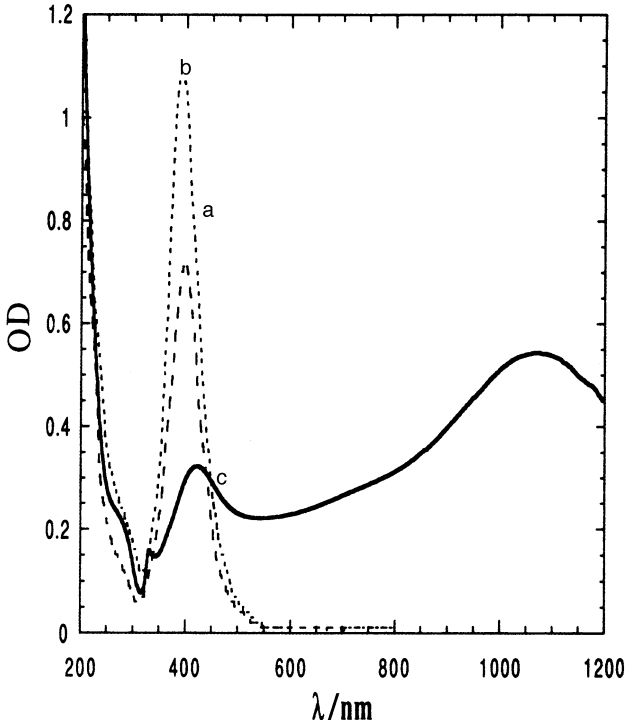

Fig. 10 Time evolution of the spectrum after 10 krad irradiation of a solution containing $[Ag^+] = 10^{-4}$ mol l^{-1}, [2-propanol] = 0.2 mol l^{-1} and [EDTA] = 5×10^{-4} mol l^{-1}, pH = 6. (*a*) Immediately after irradiation, (*b*) after 4 d, (*c*) after 8 d. (Reproduced with permission from ref. 53. Copyright 1994 Gauthier–Villars and CNRS)

reduction is assigned to the lone pair N atom electrons of the EDTA ligand and requires that the silver ions be fixed on clusters, formed by irradiation, acting as nuclei. Once the maximum value is reached, the absorption band starts decreasing and shifts towards the red while two new bands appear: a large IR band and a small peak at 330 nm [Fig. 10(*c*)]. From yellow, the solution turns bluish-gray. The whole process lasts several days. The various silver aggregates found in the different stages of this sequence were examined by TEM and QELS and then identified by microanalysis and electron diffraction. After irradiation, a micrograph revealed spherical particles with diameters of 10 to 15 nm [Fig. 11(*a*)]. The micrograph of an aged solution [Fig. 11(*b*)] shows clumps of about 100 nm in size, constituted of rather large sintered particles. The micrograph in Fig. 11(*c*) corresponds to the spectrum of Fig. 10(*c*). The clumps have disappeared and large individual particles of about 100–150 nm in size have appeared instead.

The position of the IR band obtained at the end of the experiment [Fig. 10(*c*)] depends on the ratio $R = [EDTA]/[Ag^+]$. The variation of the position of the IR band is attributed to a difference in the thickness of the triangular particles. The surface areas of the triangles have been found to be practically identical for various R values. Such an oriented growth is quite unusual. It is clear that the growth occurs preferentially in a planar way that favors the 111 surface and that EDTA plays a major role in this process. Let us note that the thickness of the final particles is approximately the diameter of the starting spherical particles.

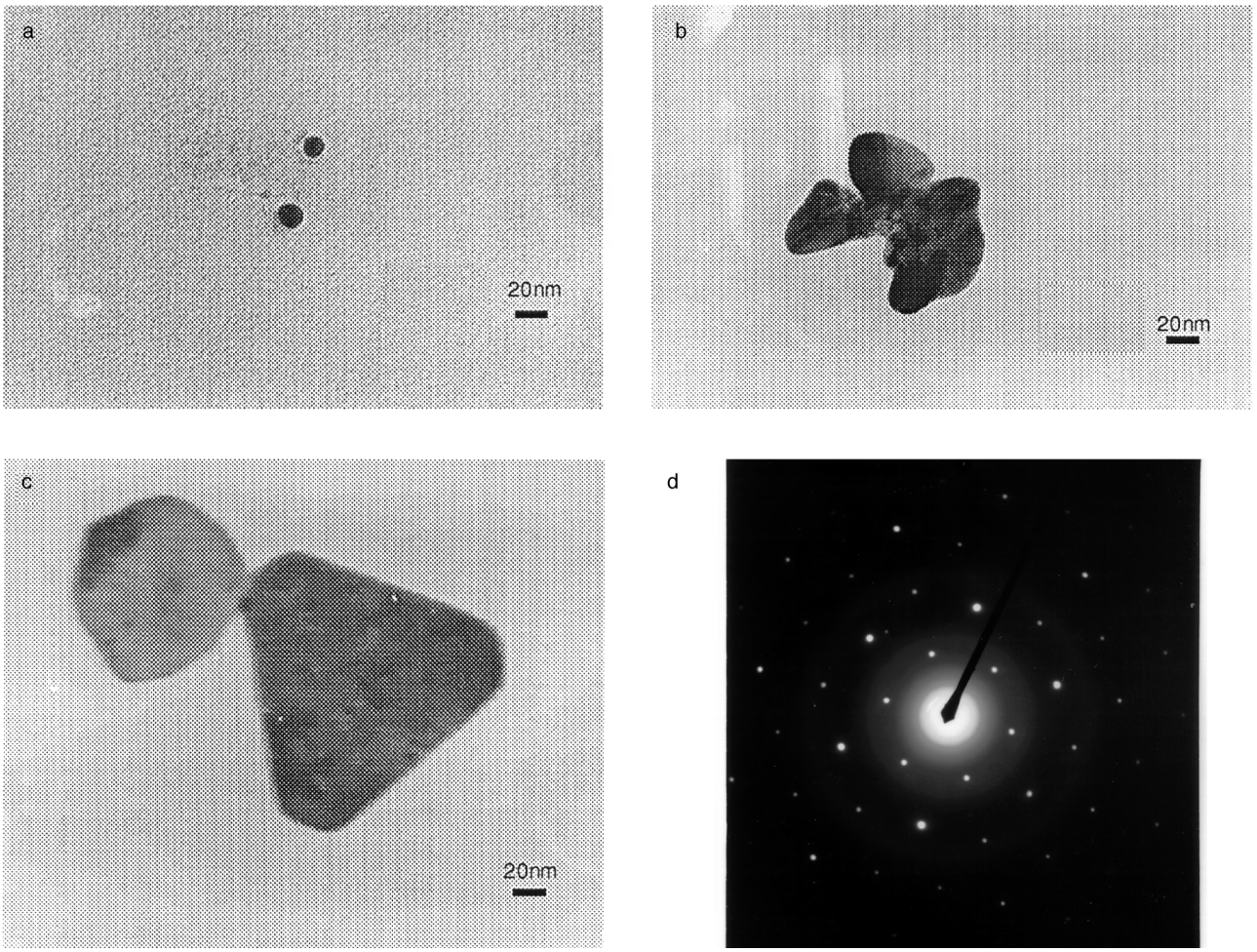

Fig. 11 (*a*), (*b*) and (*c*) TEM micrographs of samples corresponding to the spectra shown in Fig. 10(*a*), (*b*) and (*c*), respectively. (*d*) Electron diffraction patterns for the triangle in (*c*). (Reproduced with permission from ref. 53. Copyright 1994 Gauthier–Villars and CNRS)

Nickel particles–$H_2PO_2^-$. It has been shown that nickel oligomers prepared in the presence of PA in neutral or slightly basic medium and characterized by an absorption band at 540 nm may act also as a catalyst in the reduction of Ni^{2+} by hypophosphite ions. Pulse radiolysis experiments have shown that a minimum size of the oligomer is required to observe the reduction of Ni^{2+} by $H_2PO_2^-$, while free Ni^{2+} cannot be directly reduced. Under these conditions, quite large particles of nickel can be prepared with a very low radiation dose to just initiate the formation of the small supercritical nuclei, which then catalyze at their surface further reduction of Ni^{2+} by $H_2PO_2^-$ and thus are developed. The nickel particles obtained exhibit ferromagnetic properties.[38]

Gold particles–alcohol. When trivalent gold chloride $Au^{III}Cl_4^-$ is irradiated in water without any other additive at increasing doses, the reduction occurs by successive steps (reduction into the unstable bivalent state Au^{II}, then disproportionation of Au^{II} into Au^{III} and Au^{I}). However, Au^{I} ions are not reduced until trivalent gold ions have almost all been reduced, nor do they disproportionate because the redox potential involving the single atom $E°(Au^{I}/Au^{0})$ is quite negative. Thus $Au^{I}Cl_2^-$ ions accumulate.[80] With higher doses, Au^{I} ions are reduced into atoms and clusters appear. In the presence of alcohols or of preformed clusters, Au^{I} ions do not accumulate because the potential order of the (Au^{I}/Au^{0}) and (Au^{II}/Au^{I}) couples is now inverted due to complexation or adsorption, respectively. Au^{I} ions are thus allowed to disproportionate, giving rise to clusters. In addition, a very slow chemical reduction by the alcohol is found, which occurs exclusively at the surface of the clusters formed by irradiation so that all gold ions may be reduced, whatever the initial dose. As seen by AFM observations, the cluster size remains constant during the γ-irradiation and the cluster concentration increases with dose, while during the post-irradiation reduction by alcohol the size increases at a constant density of particles. The lower the dose, the larger the final size of the cubic crystallites, which may range from 10 to 500 nm, depending on the respective proportions of both types of reduction. The particles are nicely homodisperse. This system constitutes a clear example of development by a chemical reagent of small clusters radiolytically generated.

These results on development effects also demonstrate the role that dust particles could play if, at the limit, the reduction had to be totally achieved by the sole reducing agent without radiation-induced preformed clusters and if the agent was not strong enough, in contrast with e_{aq}^-, to reduce free gold ions into the zero-valent state. We suspect that this uncontrolled development is an important factor in most cases of non-reproducibility and heterodispersity observed for chemically prepared clusters.

Supported nanoclusters

One of the important applications of metal clusters is to be used as catalysts on solid supports. The radiolytic synthesis was successful in producing various supported clusters. The method consists in either (*i*) first preparing in solution nanometric metal clusters, which are then put in contact with the support (possibly by filtration) or (*ii*) irradiating directly the supporting material in contact with the solution after the ionic precursors have been adsorbed onto the support. The ionizing radiation penetrates throughout the support and forms the atoms *in situ* everywhere the ions have diffused.

Metal clusters on oxides. *Iridium clusters supported on Al_2O_3 or TiO_2.* Alumina-supported iridium clusters are efficient catalysts for hydrazine decomposition in clusters developed for spacecraft orbit and attitude control systems. To avoid poisoning by oxygen compounds, the synthesis was carried out by irradiation of an iridium solution in liquid ammonia in the presence of alumina powder.[81] When the solution contains a colloidal oxide such as TiO_2, the metal ions adsorb at the surface of the particles and after irradiation they are reduced *in situ* to the zero-valent state. The TiO_2 needles are seen by TEM but the thickness of the supported Ir layer is smaller than the resolution size (<0.8 nm). However, the cluster catalytic efficiency and the reaction mechanism may be observed by pulse radiolysis, for instance in the disproportionation reaction of the superoxide radical anion $O_2^{-\cdot}$.[82]

Platinum clusters supported on carbon. Carbon fibers and powders have also been used as supports. The interesting point is that, due to the conducting character of such materials, the metal–carbon composite can constitute electrocatalysts. Homogeneously dispersed Pt nanoparticles are obtained provided the metal is strongly anchored to the carbon surface, which is achieved through a carbon pretreatment at 930 °C under a CO_2 atmosphere. These particles are electroactive in methanol or hydrogen oxidation and in oxygen reduction.[43,83,84] However, a size increase with loading has been observed while high loadings are suitable for electrode applications (namely in fuel cells). This difficulty has been overcome by the use of CO as the ligand for preparing $Pt_x(CO)_y$ clusters (see above), which can be loaded on carbon powder up to 60 Pt wt.% while keeping a 2–3 nm size.[43,84]

Metal clusters on SnO_2. The radiolytic process has been used to graft metallic nanoaggregates onto SnO_2 transparent counter electrodes (TCE) in order to improve their electrochemical behavior. Fig. 12 presents a detectable effect as soon as the concentration of Pt ions in contact with the electrode during the irradiation reaches 10^{-4} mol l^{-1}, and a fairly good electrochemical behavior with a 10^{-3} mol l^{-1} Pt solution. The equivalent thickness has been determined by RBS to be 1 and 3 monolayers, respectively. Among various metals, iridium was shown to give the best catalytic reactivity (Fig. 12).[85] The surface concentration of grafted Ir atoms was found to be around 10^{16} atom cm^{-2}, without any loss of transparency. The electrochemical behavior of radiolytically grafted

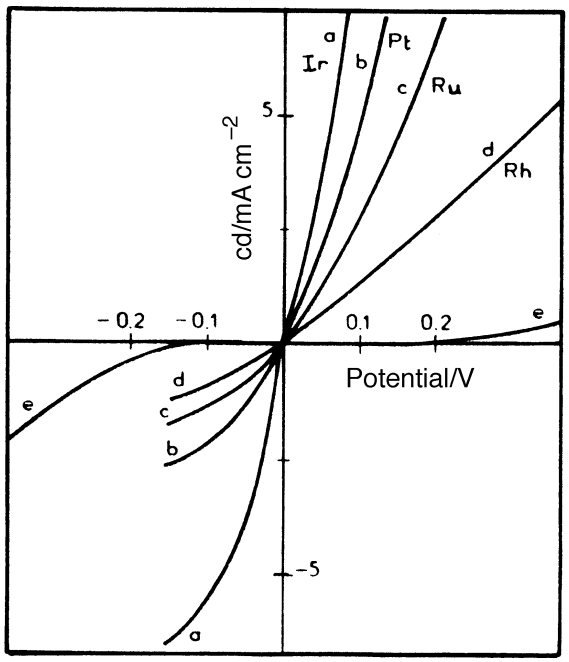

Fig. 12 Current density (cd) *vs.* voltage curves obtained from an unmodified SnO_2 transparent counter electrode or grafted with various metals in a 7 M NaI solution. $V = 0$ is the I^-/I_3^- redox potential. (Printed with permission from ref. 85. Copyright 1987 Elsevier Science)

TCE is greatly improved, approaching that of the bulk Pt electrode. No decrease in performance was observed after 1 month of operation.[86]

Silver clusters in alumino-silica gels. Silver particles have been prepared by the radiolytic method in an oxide sol, using $(EtO)_3Si{-}O{-}Al(OBu)_2$ as the oxide gel precursor.[87] The initial solution consists of an alcoholic solution of the alkoxide hydrolyzed with an aqueous solution of silver tetrafluoroborate. After γ-irradiation, the alumino-silica sol exhibits a yellow color specific of the silver aggregate absorption (Fig. 13). The average diameter of Ag particles in the oxide sol, deduced from the width of the optical absorption peak (which sharpens with increasing dose, Fig. 13), increases from 2.5 to 4.5 nm. The Ag-doped sol becomes viscous and gelatinizes within 24 h at room temperature. After one month of aging, the polycondensation substep leads to a contraction of the gel, which proceeds through the vaporization of the alcohol until the gel is completely dry and solid. Optically clear xerogels with a glassy aspect are obtained. The absorption peak is about three times more intense in the xerogel than in the initial sol due to the increase of cluster concentration but no significant change is noted in the silver particle size.

Silver oligomers on colloidal SiO_2. Colloidal supports such as small SiO_2 particles restrict interparticle diffusion of silver atoms when formed by radiolysis of the ions at their surface. The silver oligomers absorbing at 290 and 330 nm are observed by pulse radiolysis. They are stable with respect to coalescence but they are oxidized by MV^{2+}, O_2, $Cu^{2+}$and $Ru(NH_3)_6{}^{3+}$.[88]

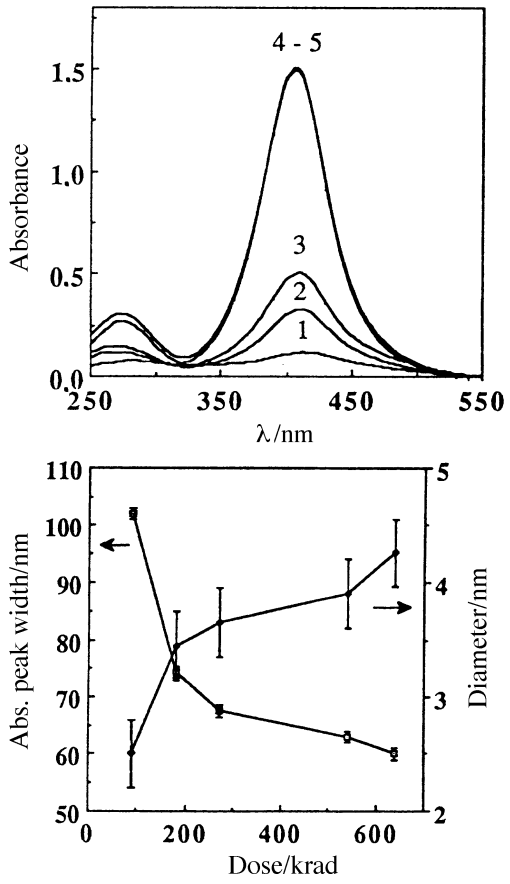

Fig. 13 Absorption spectra of silver particles in sol produced by γ-radiolysis of deaerated solutions containing 5×10^{-3} mol l^{-1} Ag^+. Top: Curves 1–5 correspond to doses of 90, 180, 270, 540 and 640 krad, respectively. $l = 2$ mm. Bottom: Plot of the optical absorption peak width (Δλ) from absorption spectra and the diameter of Ag particles deduced from Δλ *versus* radiation dose. (Reproduced with permission from ref. 87. Copyright 1991 North Holland)

Metal clusters in polymeric membranes. Positively charged metal ions easily diffuse into the cavities of a Nafion polymeric membrane by ion-exchange of the counter cations (protons or alkaline ions) of the constitutive sulfonic groups. The size of the channels and cavities is controlled by the proportion of alcohol in the aqueous solution. A pulse radiolysis study[15,89] of Ag^+ ions confined in such a membrane has demonstrated that the successive steps of the reduction and of the atom coalescence are similar to the mechanism in solution except that the diffusion, which controls the reaction rates, is slowed down by a factor of 10^4–10^5. When the Ag^+ concentration and the dose rate are low, the reverse corrosion of atoms and oligomers by the surrounding acidic medium is favored as regards the competition with the coalescence, which obeys second-order kinetics and becomes extremely slow. The overall cluster formation yield at the end is thus highly dependent on the dose rate. The kinetic analysis allowed us to determine the rate constant of the silver corrosion ($k_{corr} = 0.5$ l mol^{-1} s^{-1}) and the upper nuclearity ($n = 8$) for which this reaction occurs.[89] Similarly, nickel clusters are generated inside Nafion membrane cavities.

During irradiation of a solution of metal ions (silver, palladium or nickel) containing PVA but no other $OH^{\cdot}$ scavenger, the ion reduction occurs simultaneously with the cross-linking of the polymer.[54] Finally, after drying, the clusters formed are trapped in a polymeric film. In the case of nickel, the thin film is ferromagnetic.

Metal clusters in zeolites. Irradiation by ionizing radiation able to penetrate into a zeolite material exchanged by metal ions allows metal atoms and clusters to be generated *in situ* in the cavities.[90] The observation of irradiated faujasite (Na–Y zeolite) by optical absorption spectroscopy at increasing doses and at low silver content demonstrates the formation of two bands at 265 and 305 nm, which have been assigned to the charged trimer, $Ag_3{}^{2+}$. ESR observation after a dehydration step indicates the reduction of this species into Ag_3^0.[91]

Bi- and multimetallic clusters

Composite clusters, alloyed or bilayered, are of prominent interest as catalysts. It is therefore important to be able to select the conditions of the synthesis of composite metal clusters containing M and M′ in variable proportions, with either an alloyed or a core-shell structure. Actually, when a mixed solution of two ionic precursors M^+ and M'^+ is irradiated or chemically reduced, both situations may be encountered without clear prediction.[7]

In many cases, even though M^+ and M'^+ have generally equal probabilities to be reduced by radiolytic radicals,

$$e_{aq}{}^- + M^+ \rightarrow M^\circ \quad (2)$$

$$e_{aq}{}^- + M'^+ \rightarrow M'^\circ \quad (2')$$

a further electron transfer from the less noble metal atoms (for example M′) to the more noble metal ions M^+ systematically favors the reduction into M.

$$M' + M^+ \rightarrow (MM')^+ \rightarrow M + M'^+ \quad (17)$$

$$(M_mM'_n)^{x+} + M^+ \rightarrow (M_{m+1}M'_n)^{(x+1)+} \rightarrow (M_{m+1}M'_{n-1})^{x+} + M'^+ \quad (18)$$

If the ionic precursors are plurivalent, an electron transfer is possible as well between the low valencies of both metals, thus increasing the probability of segregation.[92] Reaction (17) has been recently observed directly by pulse techniques for some systems[93,94] and the bimetallic transient cluster sometimes identified.[93] The less noble metal ions act as an electron relay towards the noble metal ions. Thus, monometallic clusters M_n are formed first and then, when M^+ ions are exhausted, M'^+

ions are reduced afterwards at the surface of M_n. The final result is a core-shell cluster where the more noble metal M is coated by the other metal M′.

In some other cases, the intermetal electron transfer does not occur, even during hour-long irradiations.[58] The initial reduction reactions (2) or (2′) are followed by mixed coalescence:

$$M' + M \rightarrow (MM') \quad (19)$$

$$(MM') + M \rightarrow (M_2M') \quad (20)$$

and association of atoms and clusters with ions as in reactions (17) and (18):

$$(M_mM'_n)^{x+} + M^+ \rightarrow (M_{m+1}M'_n)^{(x+1)+} \quad (21)$$

$$(M_{m+1}M'_n)^{(x+1)+} + e_{aq}^- \text{ (or R)} \rightarrow (M_{m+1}M'_n)^{x+} \text{ (or } +R^+) \quad (22)$$

Then, alternating association (21) and reduction (22) reactions progressively build bimetallic alloyed clusters according to the encounter statistics, and therefore dependent on the relative initial ion abundance.[95]

A recent pulse-radiolysis study of a mixed system of monovalent cyano silver and gold ions[78] provided the first time-resolved observation of an intermetallic displacement (time range of 1 s). It is slow because it is controlled by the irreversible desorption toward the bulk of the ions released after reoxidation. The consequence is that the possible formation of an alloyed cluster or the segregation of metals in a core-shell structure depends on the kinetic competition between, on one hand, the irreversible release of the metal ions displaced by the excess ions of the more noble metal after electron transfer [reactions (17), (18)] and, on the other hand, the radiation-induced reduction of both metal ions [reactions (2), (2′), (22)], which depends on the dose rate. Once the reduction of both metal ions is complete, any further intermetallic electron transfer is no longer possible, thus suggesting that a very fast and total reduction by means of a powerful and short irradiation should produce an alloyed cluster. Indeed, such a decisive dose rate effect has been recently demonstrated.[96] However, the competition imposed by the intermetal electron transfer is more or less serious, since, depending on the metal couple, the process may not occur within an hour, or on the contrary last only minutes or even seconds.

Actually, when bilayered clusters are desired with M in the core and M′, less noble than M, in the shell (note that this order results from the proper choice of the ion complexation), radiation-induced reduction of the ion mixture must be achieved at a low dose rate to allow the equilibrium of the displacement of M′ by M^+ to be reached [reactions (17) and (18)]. The radiolytic reduction may also be applied successively in a two-step process, first to a pure M^+ solution and then to a M'^+ solution containing preformed M_n clusters, which then act as autocatalytic nuclei for growth.

In contrast, if the synthesis of alloyed clusters containing two (or even more) metals with quite different redox properties must be achieved despite a possible fast electron transfer, a high dose rate such as obtained from an electron beam must be used. An additional condition is that the total dose absorbed allows the complete reduction of all ions in order to prevent a possible post-irradiation displacement. In fact, the method has been extended successfully[97] to various couples, which as alloys exhibit improved catalytic efficiency and which could not yet be prepared through chemical reduction or γ-irradiation, due to the intermetal electron transfer. The high dose rate delivered by electron beams (or by pulsed lasers for photochemical reductions) allows an efficient competition in favor of the reduction, thus preventing a possible intermetal electron exchange, which would cause metal segregation [reactions (17), (18)]. The required reduction, achieved within a very short time, shorter than in any other chemical or electrochemical process, may be compared with a sudden non-equilibrium quenching of atoms in the lattice and results in the building of an intimately alloyed cluster with the same metal ratio as for the ionic precursors. Note that the synthesis is achieved at room temperature, far below the conditions under which diffusion of the atoms in a cluster could occur. The structure of clusters so formed, bilayered or alloyed, is therefore stable.

The control of the intermetal electron transfer even allows one to synthesize composite clusters where the *less* noble metal M′ constitutes the core: after their reduction in the monometallic solution, the M'_n clusters are mixed with a solution of M^+, and then immediately submitted to a very intense and fast irradiation, within a time much shorter than the reaction time of the electron exchange. At complete reduction exchange may no longer occur and the reverse bilayered clusters are stable.

In the following sections are described the synthesis of various bimetallic clusters, either alloyed or bilayered, and the dose rate conditions to obtain one or the other. The main techniques used to determine the structures and to differentiate between segregation or alloying of the metals were (*i*) the dose evolution of the absorption spectrum, especially when at least one of the metals presents a characteristic surface plasmon band, (*ii*) the X-ray analysis of the clusters at increasing dose, and (*iii*) the electron scattering patterns.

Core-shell particles

Bilayered Au–Ag clusters. *Bilayered Au_{core}–Ag_{shell} clusters.* Fig. 14 presents the time evolution of the optical absorption spectra of mixed solutions of $KAuCl_4$ and Ag_2SO_4 irradiated in the presence of PVA at the dose rate of 3.8 kGy h^{-1}.[96] At first the optical absorption spectrum is identical to that of pure gold clusters with a maximum at 520 nm up to a dose of 2 kGy. Local X microanalysis of clusters at partial reduction with this range of dose rate clearly indicates that gold is predominant in the particles. At increasing doses, the absorption intensity continues to increase but the single absorption maximum progressively shifts to 440 nm and the colloidal solution turns from pink to deep yellow (to compare with that of pure silver clusters at around 400 nm, inset, Fig. 14). The shift of the surface plasmon spectrum indicates that the cluster composition also changes with dose from almost pure gold clusters to clusters coated with an increasingly thick silver layer. The initially reduced silver atoms have been reoxidized in a further step through electron transfer to gold ions. Therefore, Ag^+ ions act essentially as an electron scavenger and as an electron relay toward gold ions, as long as gold ions are not almost totally reduced (Fig. 14). Then, the gold clusters formed early on adsorb most of the excess of silver ions and the silver reduction occurs at the surface of the gold particles. The final band intensity of silver-coated gold clusters corresponds to a mean extinction coefficient per Ag or Au atom of $\varepsilon_{440} = 4700$ l mol^{-1} cm^{-1} (Fig. 14). The subcolloidal solutions are then stable with time and their spectrum does not change, even in the presence of air. Electron micrographs taken from samples totally reduced indicate that the unimodal size distribution ranges from 1.5 to 12 nm.

Bilayered Ag_{core}–Au_{shell} clusters . If the precursors are gold and silver cyanide, now zero-valent silver is favored during the reduction and is formed first because gold behaves as the less noble metal, according to the respective electrode potentials in the presence of cyanide. We observe first the silver cluster band, which is then *shifted to the red* after gold reduction, thus suggesting the formation of bilayered Ag_{core}–Au_{shell} particles.[78]

Bilayered Au–Pt clusters. *Bilayered Au_{core}–Pt_{shell} clusters.* Fig. 15(top) shows the absorbance variation of an equimolar

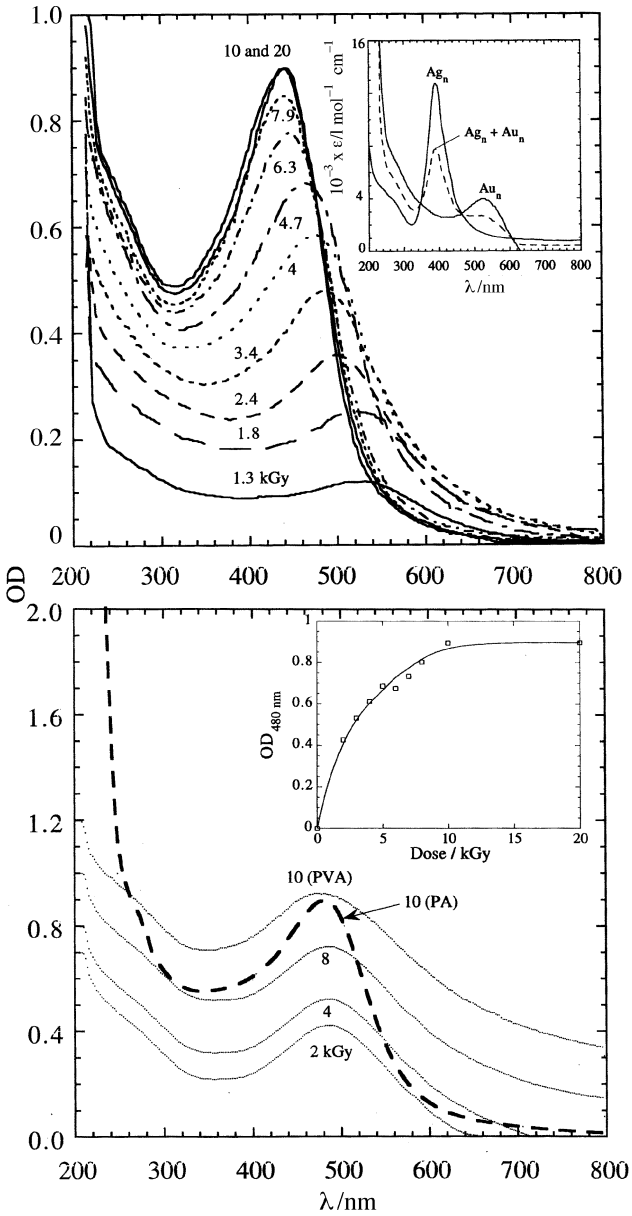

Fig. 14 Evolution with increasing dose of the absorption spectra of a mixed solution containing $[Au^{III}] = [Ag^{I}] = 5 \times 10^{-4}$ mol l^{-1}, [PVA] = 0.1 mol l^{-1}, [2-propanol] = 0.2 mol l^{-1}, pH = 10. $l = 2$ mm. Top: Dose rate of 3.8 kGy h^{-1}. Inset: (——) optical absorption spectra of pure silver or gold colloids stabilized by PVA in aqueous solutions. (– – –) Calculated absorption spectrum assuming a mixture of coexisting pure Ag_n and Au_n clusters. Bottom: Dose rate of 35 kGy h^{-1}. Dotted line: spectrum with [PA] = 0.1 mol l^{-1} at pH 4.5, other conditions the same. Inset: evolution with increasing dose of the optical density at $\lambda = 480$ nm. (Reprinted with permission from ref. 96. Copyright 1998 American Chemical Society)

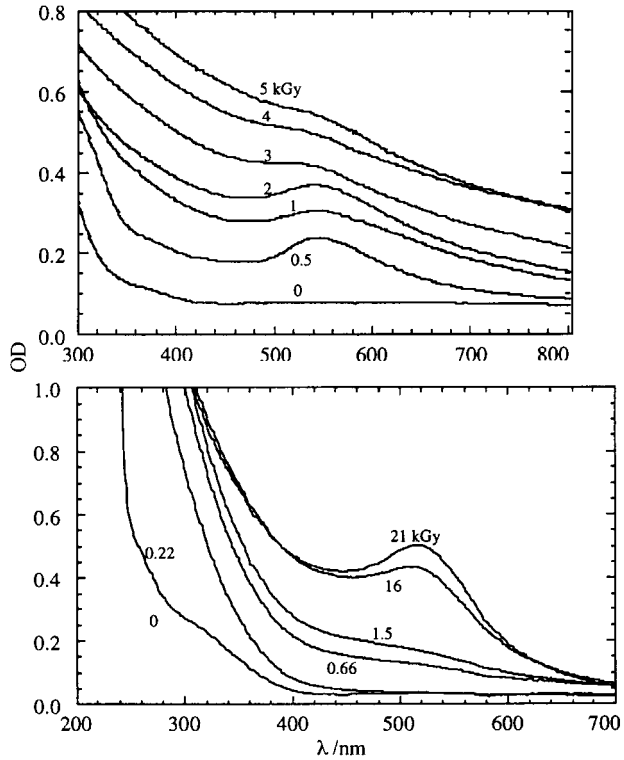

Fig. 15 Top: absorption spectra of a solution containing 5×10^{-4} mol l^{-1} of Au^{III} and 5×10^{-4} mol l^{-1} of Pt^{III} for different irradiation doses. Bottom: absorption spectra of a solution containing 5×10^{-4} mol l^{-1} of Au^{I} and 10^{-4} mol l^{-1} of Pt^{II} for different irradiation doses

mixed solution containing $HAuCl_4$ and K_2PtCl_4 with the γ dose.[98] The optical spectrum is first identical to that of pure gold clusters with a maximum at 525 nm up to a dose of 2 kGy, corresponding to the nearly total reduction of gold. EDS observation confirms the absence of platinum in clusters at this stage. The absorption intensity continues to increase with dose, but the 525 nm maximum progressively disappears, thus indicating a progressive coating of gold clusters by platinum (bilayered Au_{core}–Pt_{shell} particles). The final spectrum is almost similar to that of platinum clusters except for a weak shoulder around 525 nm due to the gold core (Fig. 15) because the platinum layer is thin. Both metals are now observed by EDS. The preferential formation of gold clusters is found as it was also the case in chemical reduction and is favored by the more noble character of Au compared to Pt. At least, it has been shown that Pt^{II} slowly reduces Au^{III} into gold clusters and that these clusters then catalyze the reduction.

We checked whether increasing the dose rate could prevent the intermetal electron transfer and allow the formation of alloyed Au–Pt particles. The spectral evolution with the dose clearly shows that even at the high dose rate of an electron beam the gold clusters are still formed first (bilayered Au–Pt clusters). In fact, both ions in this system are multivalent and the possible electron transfer reactions between low valency free ions could be much faster than with a cluster. Therefore, the dose rate used was not high enough to ensure the total reduction faster than these processes, thus preventing the formation of alloyed Au–Pt particles in solution.

Bilayered Pt_{core}–Au_{shell} clusters. By a two-step reduction, it is possible to obtain bilayered particles with the reverse order compared to that spontaneously obtained by irradiating the ion mixture with one-step irradiation as above. A few minutes after addition of $Au^{III}Cl_4^-$ ions to a sol of Pt clusters (Fig. 15) shoulders appear around 530 and 260 nm. The first one corresponds to the plasmon band of gold; the second indicates the formation of $Pt^{IV}Cl_6^{2-}$ ions. The chemical reduction of gold at the surface of platinum particles allows the formation of bilayered clusters. Note that the platinum is finally not totally dissolved; therefore, the bilayered particles are made of platinum in the core and gold at the surface.

The same order of metals is obtained by one-step irradiation using a mixed solution containing initially $Au^{I}(CN)_2^-$ which has a very low redox potential and $Pt^{II}Cl_4^{2-}$ (PVA). At low doses, the absorption spectrum of platinum clusters is present without the plasmon band of gold but superimposed with non-reduced $Au^{I}(CN)_2^-$ bands at 232 and 242 nm, thus indicating that platinum ions reoxidize early formed gold atoms. At the dose of 20 kGy, which is sufficient to reduce all the ions of the mixed solution, the maximum has shifted to 520 nm due to the reduction of gold ions at the surface of early formed platinum clusters. Therefore, when using $Au(CN)_2^-$ as the gold ion precursor, the final structure of the

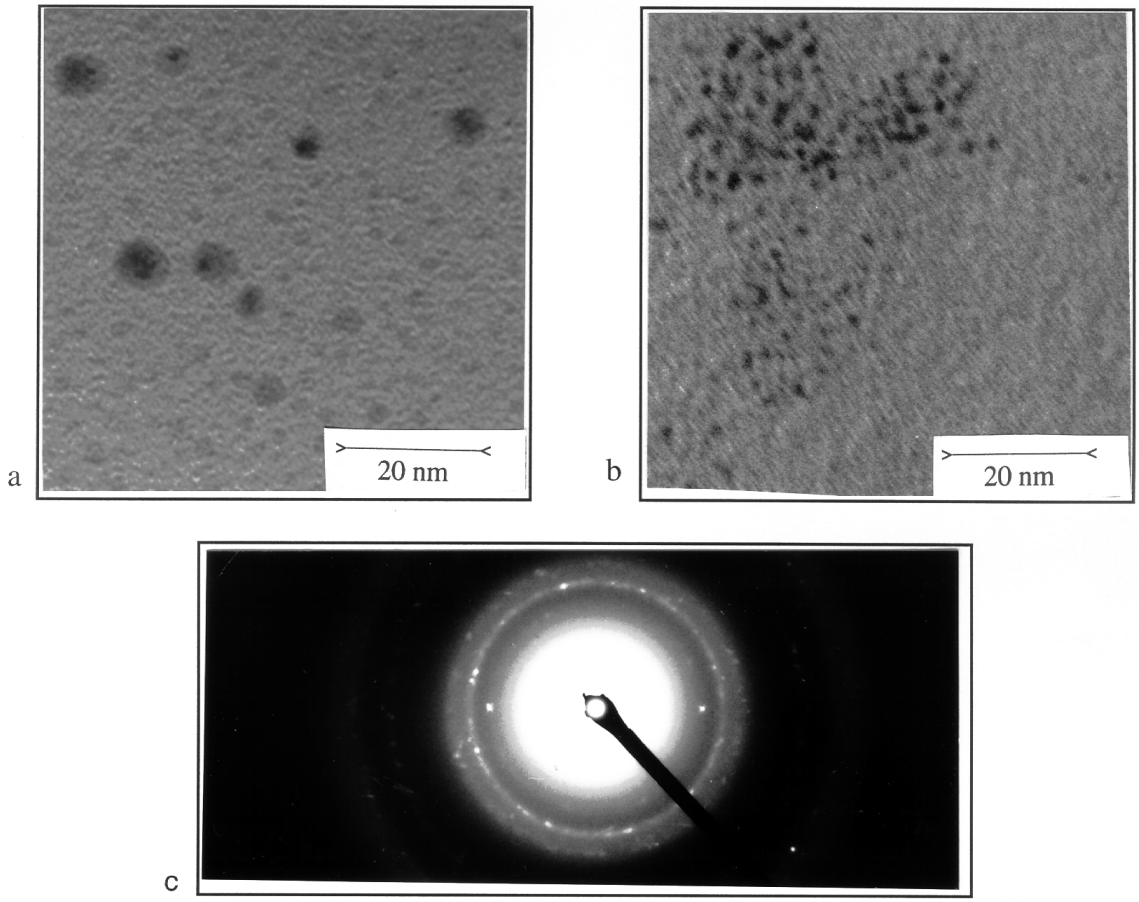

Fig. 16 (*a*), (*b*) Micrographs and (*c*) electron diffraction pattern of Ag–Au (50 : 50) bimetallic particles stabilized by PVA or PA and obtained at different dose rates. (*a*) Dose rate = 35 kGy h^{-1}, dose = 20 kGy (PA), (*b*) dose rate = 7.9 MGy h^{-1}, dose = 30 kGy (PVA). (*c*) Diffractogram of the sample corresponding to micrograph (*a*). Note the presence of two central intense spots, corresponding to the lattice distance d_{110}, due to the existence of a perfectly ordered alloy of A_3B stoichiometry (A = Ag or Au). (Reprinted with permission from ref. 96. Copyright 1998 American Chemical Society)

bimetallic Pt–Au clusters is reversed compared to that obtained with $Au^{III}Cl_4^-$.

Ag–Cu and Au–Ag–Cu. When a mixed solution of silver and copper sulfate is γ-irradiated at increasing dose, the observed absorption spectrum (λ_{max} = 400 nm) is first that of monometallic silver clusters. The silver ion reduction is favored by the fast electron transfer from Cu^+ to Ag^+.[99] After complete reduction of Ag^+, the band progressively shifts to the red because reduced copper is now coating Ag_n.[100] In air, this copper shell is oxidized so that only the silver core remains. Similar copper-coated silver clusters are formed when the precursor ions are complexed by poly(ethyleneimine).[101] If the solution contains the ions $Au^{III}Cl_4^-$, Ag^+ and Cu^{2+}, they are reduced successively in this order because this corresponds to the decreasing order of redox potentials. Thus, at increasing dose, the spectrum of Au_n appears first (λ_{max} = 520 nm). Then, a blue shift is observed corresponding to the coating of gold clusters by silver (λ_{max} = 400 nm), and in a third step another shift backwards to the red corresponds to the external coating by copper (λ_{max} = 570 nm). Thus, the final trimetallic clusters contain a gold core coated by two successive layers of silver and copper.[102]

Alloyed clusters

The process of the progressive building of alloyed clusters results from coalescence between reduced atoms and clusters, and also from the *in situ* reduction of mixed charged particles [reaction (22)], both processes resulting from the encounter statistics.[96] Actually, coalescence, association with ions and radiolytic reduction must occur out of the equilibrium concerning the mutual electron transfer reactions between metals. Once this quenching radiolytic reduction has consumed all the ions, the intermetal displacement process is excluded.

Depending on the rate of the competitive intermetal electron transfer, alloying of metal atoms may occur spontaneously, even at low reduction rate (γ-irradiation with low dose rate),[58] or may require higher γ-dose rates,[96,97] or may even be obtained only through a short and intense irradiation provided by an electron accelerator. In extreme cases, the electron transfer is achieved within times shorter than the irradiation time used (a few seconds in our case) and metals are segregated in spite of the very fast reduction.[98] The following systems are described in increasing order of dose rate required to prevent metal displacement and segregation.

Alloyed Cu–Pd, Ni–Pt and Ag–Pt clusters. In some systems, γ-irradiation of a mixed solution of two metal precursor ions yields spontaneously alloyed bimetallic clusters, even at moderate dose rate. Their structure as analyzed by electron diffraction is clearly that of solid solutions. Moreover, superlattice reflections imply ordered atomic arrangements. For example, the sol formed when irradiating a mixed $CuSO_4$ and $PdCl_2$ solution (PVA) is dark green (instead of pink for Cu or brown for Pd clusters). Superlattices corresponding to Cu_3Pd and CuPd fcc structures, respectively, are observed for Cu^{2+}–Pd^{2+} (90 : 10) and Cu^{2+}–Pd^{2+} (50 : 50) mixtures.[58] Similar Ni_3Pt superlattices (in Ni^{2+}–$PtCl_4^-$ 90 : 10) were found.[54,55] Nickel is also easily alloyed with ruthenium. Although monometallic iron clusters are unstable in the irradiated solution, a ferromagnetic alloy of Cu–Fe may be formed in the mixed Cu^{2+}–Fe^{3+} solution.

Irradiating aqueous solutions containing both Ag_2SO_4 and K_2PtCl_4 at low γ-dose rates leads to intermetallic clusters of various sizes depending on the stabilizing agent. The alloyed character of such sols is demonstrated at different precursor ratios by the intensity of the absorption spectrum which increases with dose without any change in spectral shape.[103] In Ag_{1-x}–Pt_x, for x values as low as 0.1–0.2, the specific plasmon band of silver disappears. In the case of PA (pH 4) used as stabilizer, the cluster diameter is 1.5 nm. It is interesting to note that the alloyed Ag–Pt clusters are much smaller than the monometallic Ag ones and close in size to Pt clusters under comparable conditions, even if the Pt content is low.

Alloyed Ag–Au clusters. When the same solutions of $KAuCl_4$ and Ag_2SO_4 as above are γ-irradiated at the dose rate of 35 kGy h^{-1}, the shape of the spectrum does not change with dose while the intensity progressively increases (Fig. 14, bottom), in contrast with the results at lower dose rate [Fig. 14, top].[96] The same evolution with dose is also found when the sample is irradiated by an electron beam at the dose rate of 7.9×10^3 kGy h^{-1}. The new band is now centered at 480 nm, an intermediate value between 400 nm (Ag_n) and 520 nm (Au_n). The maximum absorbance at complete reduction corresponds to an extinction coefficient of $\varepsilon_{480} = 4500$ l mol^{-1} cm^{-1} per metal atom. This identical spectrum shape at any dose therefore testifies to the existence of the same strong interaction between the two metals, which are alloyed in a constant proportion from the lowest doses and consequently identical to that of the ionic precursors. The particle size increases with dose, thus explaining the rise of a red component in the spectrum. When the reduction of Au^{III}–Ag^{I} solutions is achieved in the presence of PA polymer, instead of PVA, the optical absorption spectrum is quite similar in position and intensity of the band, except that in the 600–800 nm domain the light scattering is much less important than with PVA (Fig. 14), thus suggesting that the mean size of clusters stabilized by PA is smaller as usually observed also for monometallic particles.[88] Moreover, the TEM images obtained from alloyed gold–silver solutions after irradiation at a high dose rate (7.9 MGy h^{-1}) show that, despite the less strong stabilizing character of PVA, isolated and homodisperse clusters 2–3 nm in diameter are found [Fig. 16(*b*)], markedly smaller than at 35 kGy h^{-1} with PA [Fig. 16(*a*)]. This dose rate effect has been also observed for monometallic clusters. Indeed, sudden generation of a high concentration of isolated atoms at high dose rate and thus the formation by coalescence of more numerous and smaller nuclei is favored compared to the reduction *in situ* of adsorbed ions at the surface of clusters, which occurs mostly at low dose rate and contributes to development of less numerous growth centers.

The same evolution with dose has been studied for various values of the x fraction of Au ions in the initial solution. Surface plasmon spectra at x values for which optical data are available[50,51] have been calculated from the Mie model. The dependence on x of the calculated values of λ_{max} and ε_{max} are presented in Fig. 17(*a*) and (*b*), respectively, and compared with the corresponding experimental data. Similar calculations have been done[104] for the alloy $Ag_{1-x}Au_x$.

Silver and gold crystallize with the same fcc lattice and very similar a_o parameters (Ag: 0.4086 nm and Au: 0.4078 nm), so that not much difference can be expected from the diffraction patterns of alloyed or non-alloyed particles. However, additional features may appear in the case of superlattices in which a perfectly ordered arrangement of the two metals is found over a long-distance range. Fig. 16(*c*) emphasizes such a phenomenon: from a Ag–Au (PA) sample analyzed on a single cluster, two new intense spots are superimposed on the usual Debye–Scherrer diagram. They correspond to the d_{110} distance, which is absent in a random solid solution, so that the

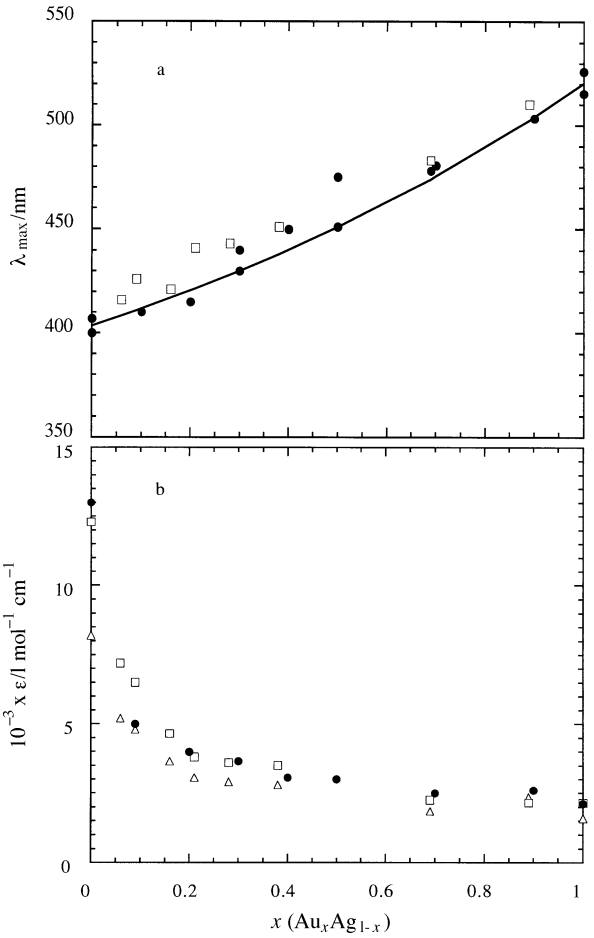

Fig. 17 (*a*) Maximum wavelength of the gold–silver plasmon band as a function of the mole fraction of gold at the dose rate 7.9×10^3 kGy h^{-1} and dose 20 kGy. Total metal concentration = 10^{-3} mol l^{-1}, [PVA] = 0.1 mol l^{-1}, [isopropanol] = 0.2 mol l^{-1}. (●) Experiment, (□) calculated values deduced from Ripken's optical data (——) eqn. (9) of ref. 94. (*b*) Extinction coefficient at the maximum of the gold–silver plasmon band as a function of the mole fraction of gold. (●) Experiment, (□) eqn. (5) of ref. 96 with $r = 5$ nm, (△) eqn. (5) of ref. 96 with $r = 3$ nm. (Reprinted with permission from ref. 96. Copyright 1998 American Chemical Society)

Au_3Ag superlattice is clearly detected. The same structure has been found in particles contained in an irradiated 0.68 : 0.32 Au^{III}–Ag^{I} (PA) sample.

It has been shown above that when mixed solutions of monovalent silver and gold cyanide are γ-irradiated, even at the high dose rate of 35 kGy h^{-1}, bilayered gold-coated silver clusters are formed.[79] However, with an electron beam delivering 7.9 MGy h^{-1}, and allowing a much faster and complete reduction, the absorption spectrum is quite different. The maximum is at 420 nm and the extinction coefficient per atom of the alloyed cluster is $\varepsilon_{420}(AgAu)_{n,\,CN^-} = 2250$ l mol^{-1} cm^{-1}.[96]

Another way to favor the statistical reduction leading to alloyed particles is to let the clusters grow more rapidly, before any observable intermetal transfer, and consequently to let their redox potential increase in order to lower the risk of displacement. This can be achieved through a fast chemical reduction by a donor D at a nucleus formed by irradiation as in the development process (see above). The reaction competing with the intermetal exchange is now the chemical reduction, which can be very fast provided nuclei are present. In a pulse radiolysis study, the transient reduced viologen formed by an electron pulse has been observed to react with the small alloyed gold–silver clusters and the developed

alloyed clusters are stable towards segregation. Moreover, the redox behavior of such alloyed clusters is almost the same as that of the more noble metal (silver in cyanide environment).[79]

Alloyed Ag–Pd clusters. Clusters have been synthesized by γ-irradiation-induced reduction of aqueous solutions of metal sulfate salts with different Ag^{I}–Pd^{II} ratios in the presence of polyacrylic acid.[105] The maximum of the surface plasmon spectra of pure silver or palladium clusters are at 400 nm and around 205 nm, respectively. During the evolution with dose of the optical absorption spectra of a mixed solution of Ag_2SO_4 and $PdSO_4$ (Ag^{I} fraction $x = 0.94$) irradiated at the dose rate 35 kGy h^{-1} in the presence of PA, the band intensity progressively increases but the shape is unchanged (Fig. 18), in particular at the shoulder at 360 nm. The features of the optical spectrum evolution strongly suggest that the cluster composition is the same from the beginning to the end of the cluster growth and that the clusters formed are alloyed throughout the cluster volume with a composition close to that of the ionic precursors.

The UV/VIS spectra of Ag_x–Pd_{1-x} clusters with lower x values were studied similarly at different doses. As x decreases, the maximum wavelength of the shoulder is blue-shifted. In Fig. 19 are plotted the λ_{max} values observed *versus* x and the values calculated according to Mie theory for alloyed clusters, which fit nicely. At $x = 0.55$, the electron diffractograms corresponding to a dense cluster area present the typical Debye–Scherrer patterns of solid solutions with, quite rarely, extra spots testifying to the presence of superlattices such as Ag_3Pd, thus confirming that intimately alloyed clusters are formed.

Supported multimetallic clusters

Metal clusters on metal electrodes. The radiolytic method was also used to graft metal nanoaggregates upon anodes or cathodes involved in the chlorine-soda process.[106] In both cases important overpotentials are usually measured on unmodified electrodes. The electrocatalytic efficiency of bimetallic nanoparticles (such as Pt–Ru and Ni–Ru), once grafted onto bulk metal electrodes (Ti or Ni), has been investigated. As a synergistic effect, a drastic decrease of the overpotential is observed when Pt and Ru are alloyed in a 2 : 1 atomic ratio.

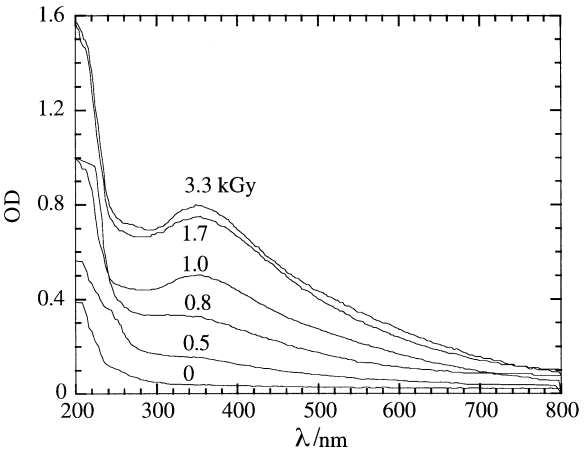

Fig. 18 Evolution with irradiation dose of the optical absorption spectrum of a mixed solution of Ag_2SO_4 and $PdSO_4$ (Ag^{I} fraction $x = 0.94$). Total concentration of metal ions is 10^{-3} mol l^{-1}, [2-propanol] = 0.2 mol l^{-1}, [PA] = 0.1 mol l^{-1}, pH 2 (H_2SO_4). Doses from 0 (before irradiation) to 3.3 kGy. (Reproduced with permission from ref. 105. Copyright 1997 Springer Verlag)

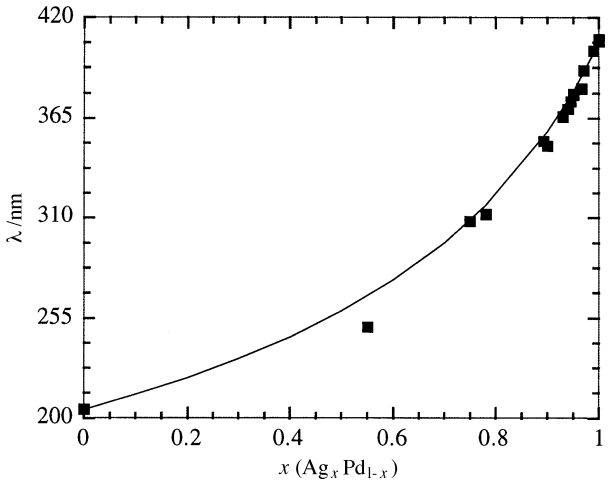

Fig. 19 Dependence of the maximum wavelength of the surface plasmon band on the composition x of the mixed ion Ag^{I}–Pd^{II} solution at complete reduction. Other conditions as in Fig. 18. (■) Experimental data. Curve: calculated data according to eqn. (4) of ref. 103. (Reproduced with permission from ref. 105. Copyright 1997 Springer Verlag)

Metal clusters on silver halide emulsions. As shown by numerous examples, the reduction of ions by an electron donor is catalyzed by small clusters and does not occur directly except for extremely strong reducing agents. This specificity is used in the photographic development process.[5] However, the silver halide support affects, by shifting it towards more positive values, the redox potential for a given nuclearity.[107] The electron transfer reactions between silver clusters at the surface of silver chloride and reduced and oxidized forms of developer agents were observed.[108] Particularly, special diffusion transfer processes require the diffusion of the silver ions of the positive image and their catalytic reduction around added development centers such as metal clusters small enough to ensure a high resolution and to be active without loss of transparency. Added γ-induced silver clusters have an interesting efficiency, but alloyed clusters of Au–Cu and Ni–Pt[109] and particularly of Ag–Au, Ag–Cu and Ag–Cu–Pd, prepared under high dose rate conditions, exhibit the best activity.[97]

CO-stabilized Pt–Ru and Pt–Ru–Sn clusters on carbon. It has been seen above that Pt–carbon composites are of high interest in making electrodes for fuel cells.[43,110] In order to enhance the methanol electrooxidation currents at lower potentials and to extend the catalyst lifetime, Pt is alloyed with other metals such as Ru or Sn. Bimetallic Pt–Ru, Pt–Sn and trimetallic Pt–Ru–Sn, stabilized by CO in solution, are prepared by electron beam reduction at a high dose rate to enhance the probability of alloying. These clusters may be easily impregnated as nanoparticles onto carbon powder at high loading (up to 40 Pt wt.%) without noticeable increase in particle size (in the 1–4 nm range). The optimized compositions for Pt–Ru–Sn 70 : 15 : 15 and 70 : 20 : 10 (atomic ratio) exhibit a current density of 650 mA (mg Pt)$^{-1}$ at 0.55 V_{SHE} [to be compared with pure platinum: 120 mA (mg Pt)$^{-1}$ at 0.55 V_{SHE}] (Fig. 20).[110] The conclusion on the alloyed character of the bimetallic, *a fortiori* trimetallic clusters, is deduced from their relative catalytic efficiency. Actually, mixed clusters synthesized by γ-radiolysis are less active than those prepared by electron beam irradiation, which suggests that the marked improvement observed in the catalytic properties of the latter is explained by an intimate alloying of the metals.

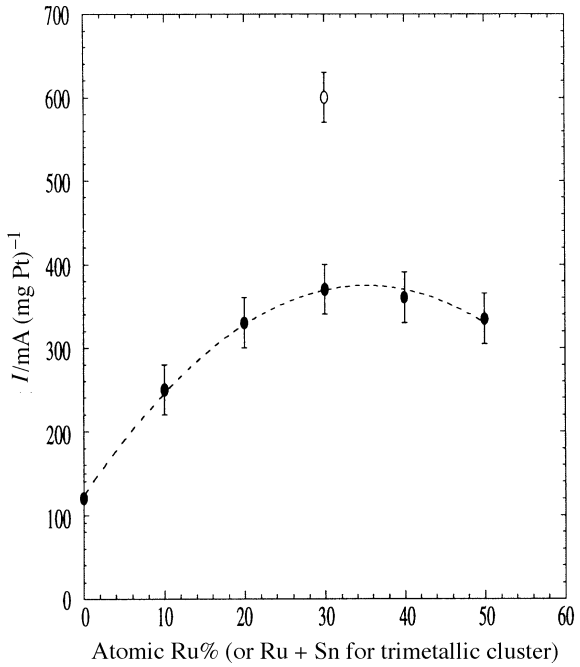

Fig. 20 Catalytic activities of mono- and multimetallic CO-stabilized clusters supported on carbon, measured by cyclic voltammetry. Potential: -0.55 V_{SHE} in 1.5 mol l^{-1} H_2SO_4 and 1 mol l^{-1} MeOH at 60 °C. The trimetallic cluster composition is $Pt_{0.70}Ru_{0.15}Sn_{0.15}$

Conclusions

Radiolysis of solutions containing metal ions has allowed the emergence of the knowledge on the very special properties of free atoms and oligomer clusters in solution and on their nuclearity-dependent redox potentials. It has been emphasized that, due to the highly negative redox potential of single atoms (even for noble metals), their reduction with mild chemical reductants cannot start by itself and requires adsorption of ions either onto the walls or onto dust particles (an exception has to be made in the case of some complexed metal ions whose potential is drastically increased). Consequently, the chemical reduction process is difficult to control and yields heterodisperse particles. In contrast, radiolysis generates extremely powerful reducing radicals able to overcome the thermodynamic barrier for the reduction of single metal atoms in solution, even at room temperature. In the following step of atom coalescence, the dose rate is the key to particle growth. It regulates the generation of the new reduced units while coalescence occurs as a second-order diffusion-controlled process, depending on the nuclei concentration, which is itself directly related to the dose rate. In this way, the final size of particles, limited by the use of a size-limiting agent (polymer, ligand, support), exhibits a remarkable homodispersity.

When two or more metal ions are present, the very first reduction event occurs in a statistical way among the metal ion population, according to their relative abundance and the scavenging rate constants of the radiolytic species. In the second step, the intermetal electron transfer competes with coalescence so that the electron transfer rate determines the final structure of the particles: either alloyed or layered (core-shell). The relevant parameter is then the dose rate to intermetal transfer rate ratio. The intermetal transfer rate has been found to be extremely variable from one couple of metals to another so that different situations could be observed and dose rates required to get alloyed clusters have been found to differ by several orders of magnitude. The alloyed structure for bimetallic particles such as Cu–Pd, Ni–Pt and Ag–Pd has been obtained even at low dose rates (γ-irradiation requiring hours). For the Au–Ag system (Cl^- ligand), the synthesis of the alloyed clusters must be achieved within minutes by the use of a higher γ-dose rate. For Ag–Cu or Au–Ag (CN^- ligand), alloying requires the quenching reduction to be performed within seconds by using a powerful electron accelerator. Up to now, even these last conditions were not sufficient for the Au–Pt system. It would be interesting to further increase the radiation dose rate to check the possibility of forming alloyed Au–Pt particles.

The applications of radiolytically prepared metal particles concern two main fields. The first one is catalysis for which interest lies in various specificities accessible by the radiation-induced reduction method: (*i*) small size and homodispersity, (*ii*) highly loaded supports and (*iii*) alloying. The double character, reducing and oxidizing, of small clusters enables them to act as a catalytic electron relay between an electron donor and an electron acceptor, which otherwise would react together too slowly. The catalytic efficiency of metal clusters is thermodynamically controlled by an appropriate redox potential, which must be intermediate between those of the donor and of the acceptor.[6,95]

The second field addressed is the development of very tiny nuclei into much larger sized particles through chemical reduction at the surface of the nuclei in a self-catalytic process. Photographic development and other processes related to photography are the best examples of such reactions.

References

1 M. O. Delcourt and J. Belloni, *Radiochem. Radioanal. Lett.*, 1973, **13**, 329.
2 M. Haissinsky, in *Radiation Chemistry*, ed. J. Dobo and P. Hedvig, Akad. Kiado, Budapest, 1972, vol. II, pp. 1353–1365.
3 N. Basco, S. K. Vidyarthi and D. C. Walker, *Can. J. Chem.*, 1973, **51**, 2497.
4 A. Henglein, *Ber. Bunsenges. Phys. Chem.*, 1977, **81**, 556.
5 (*a*) M. Mostafavi, J. L. Marignier, J. Amblard and J. Belloni, *Radiat. Phys. Chem.*, 1989, **34**, 605; (*b*) *Z. Phys. D: Atoms, Molecules, Clusters*, 1989, **12**, 31.
6 J. Khatouri, M. Mostafavi and J. Belloni, in *Photochemistry and Radiation Chemistry. Complementary methods for the study of electron transfer*, ed. J. Whishart and D. Nocera, American Chemical Society, Washington, DC, 1998.
7 Belloni, J., *Curr. Opinion Colloid Interface Sci.*, 1996, **1**, 184.
8 J. Belloni, J. Amblard, J. L. Marignier and M. Mostafavi, in *Clusters of Atoms and Molecules*, ed. H. Haberland, Springer, Berlin, 1994, vol. II, pp. 290–311.
9 A. Henglein, *J. Phys. Chem.*, 1993, **97**, 5457; *Ber. Bunsenges. Phys. Chem.*, 1995, **99**, 903.
10 J. S. Bradley, in *Clusters and Colloids*, ed. G. Schmid, VCH, New York, 1994, pp. 459–544.
11 J. H. Baxendale and F. Busi., *The Study of Fast Processes and Transient Species by Electron Pulse Radiolysis*, NATO ASI Series 86, D. Reidel, Town 1982.
12 G. V. Buxton, Q. G. Mulazzini and A. B. Ross, *J. Phys. Chem. Ref. Data*, 1995, **24**, no. 3.
13 J. Elliott and A. S. Simon, *Radiat. Phys. Chem.*, 1984, **24**, 229.
14 H. A. Schwarz and R. W. Dodson, *J. Phys. Chem.*, 1989, **93**, 409.
15 O. Platzer, J. Amblard, J. L. Marignier and J. Belloni, *J. Phys. Chem.*, 1992, **96**, 2334.
16 A. M. Koulkes-Pujo and S. Rashkov, *J. Chim. Phys.*, 1967, **64**, 534; *ibid.*, 1968, **65**, 911.
17 M. Mostafavi and J. Belloni, *Recent Res. Development Phys. Chem.*, 1997, **1**, 459.
18 A. Henglein, *J. Phys. Chem.*, 1979, **83**, 2209.
19 C. D. Jonah, M. S. Matheson and D. Meisel, *J. Phys. Chem.*, 1977, **81**, 1805.
20 R. Rafaeloff, Y. Haruvy, J. Binenboym, G. Baruch and L. A. Rajbenbach, *J. Mol. Catal.*, 1983, **22**, 219.
21 M. Graetzel, *Acc. Chem. Res.*, 1981, **14**, 376.
22 B. G. Ershov, *Russ. Chem. Bull.* (*Engl. Transl.*), 1994, **43**, 16.
23 T. Sosebee, M. Giersig, A. Holzwarth and P. Mulvaney, *Ber. Bunsenges. Phys. Chem.*, 1995, **99**, 40.
24 M. Mostafavi, N. Keghouche, M. O. Delcourt and J. Belloni, *Chem. Phys. Lett.*, 1990, **167**, 193.
25 A. Henglein, *Chem. Phys. Lett.*, 1989, **154**, 473.
26 K. Kurihara, J. Kizling, P. Stenius and J. H. Fendler, *J. Am. Chem. Soc.*, 1983, **105**, 2574.

27 J. Belloni, F. Billiau, P. Cordier, J. Delaire and M. O. Delcourt, *J. Phys. Chem.*, 1978, **82**, 532.
28 A. Henglein, T. Linnert and P. Mulvaney, *Ber. Bunsenges. Phys. Chem.*, 1990, **94**, 1449.
29 M. Mostafavi, M. O. Delcourt and G. Picq., *Radiat. Phys. Chem.*, 1992, **41**, 453.
30 M. Mostafavi, M. O. Delcourt, N. Keghouche and G. Picq, *Radiat. Phys. Chem.*, 1992, **40**, 445.
31 M. Mostafavi, N. Keghouche and M. O. Delcourt, *Chem. Phys. Lett.*, 1990, **169**, 81.
32 N. Keghouche, M. Mostafavi, M. O. Delcourt and G. Picq, *J. Chim. Phys.*, 1993 **90**, 777.
33 S. Remita, J. M. Orts, J. M. Feliu, M. Mostafavi and M. O. Delcourt, *Chem. Phys. Lett.*, 1994, **218**, 115.
34 B. Keita, L. Nadjo, C. de Cointet, J. Amblard and J. Belloni, *Chem. Phys. Lett.*, 1996, **249**, 297.
35 A. Henglein, B. G. Ershov and M. Malow, *J. Phys. Chem.*, 1995, **99**, 14129.
36 J. Khatouri, M. Mostafavi, J. Amblard and J. Belloni, *Chem. Phys. Lett.*, 1992, **191**, 351.
37 B. G. Ershov and N. L. Sukhov, *Radiat. Phys. Chem.*, 1990, **36**, 93.
38 M.-Z. Lin, Thesis, Université de Paris-Sud, Orsay, 1996. M.-Z. Lin and J. L. Marignier., unpublished work.
39 H. Remita, R. Derai and M. O. Delcourt, *Radiat. Phys. Chem.*, 1991, **37**, 221.
40 H. Remita, Thesis, Université de Paris-Sud, Orsay, 1990.
41 G. Longoni and P. Chini, *J. Am. Chem. Soc.*, 1976, **98**, 7225.
42 B. Le Gratiet, H. Remita, G. Picq and M. O. Delcourt, *Radiat. Phys. Chem.*, 1996, **47**, 263.
43 B. Le Gratiet, H. Remita, G. Picq and M. O. Delcourt, *J. Catal.*, 1996, **164**, 36.
44 K. Torigoe, H. Remita, G. Picq, J. Belloni and D. Bazin., unpublished work.
45 H. Remita, R. Derai and M. O. Delcourt, *J. Chim. Phys.*, 1991, **88**, 845.
46 M. M. Bettahar and M. O. Delcourt, *Radiat. Phys. Chem.*, 1988, **32**, 779.
47 R. Derai, H. Remita and M. O. Delcourt, *Radiat. Phys. Chem.*, 1991, **38**, 483.
48 G. Schmid, R. Pfeil, R. Boese, F. Banderman, S. Meyer, G. H. M. Calis and J. W. A. van der Velden, *Chem. Ber.*, 1981, **114**, 3634.
49 G. Schmid, *Structure and Bonding*, Springer-Verlag, Berlin, 1985.
50 U. Kreibig and M. Vollmer, *Optical Properties of Metal Clusters*, Springer, Berlin, 1995.
51 J. A. Creighton and D. J. Eadon, *J. Chem. Soc., Faraday Trans.*, 1991, **87**, 3881.
52 S. Underwood and P. Mulvaney, *Langmuir*, 1994, **10**, 3427.
53 S. Remita, M. Mostafavi and M. O. Delcourt, *New J. Chem.*, 1994, **18**, 581.
54 J. L. Marignier, Thesis, Université de Paris-Sud, Orsay, 1987.
55 J. Belloni, J. L. Marignier, M. O. Delcourt and M. Minana, *US Pat.* 4 629 709, 1986; *CI Pat.* 4 745 094, 1987.
56 B. G. Ershov, N. L. Sukhov and D. I. Troistskii, *Russ. J. Phys. Chem.* (*Engl. Transl*), 1994, **68**, 734.
57 G. Mills and A. Henglein, *Radiat. Phys. Chem.*, 1985, **26**, 391.
58 J. L. Marignier, J. Belloni, M. O. Delcourt and J. P. Chevalier, *Nature* (*London*), 1985, **317**, 344.
59 J. L. Marignier and J. Belloni, *J. Chim. Phys.*, 1988, **85**, 21.
60 J. Von Pukies, W. Roebke and A. Henglein, *Ber. Bunsenges. Phys. Chem.*, 1968, **72**, 842.
61 R. Tausch-Treml, A. Henglein and J. Lilie, *Ber. Bunsenges. Phys. Chem.*, 1978, **82**, 1335.
62 M. O. Delcourt, J. Belloni, J. L. Marignier, C. Mory and C. Colliex, *Radiat. Phys. Chem.*, 1984, **23**, 485.
63 Gosh-Mazumdar and E. J. Hart, *Int. J. Radiat. Phys. Chem.*, 1969, **1**, 165.
64 A. Henglein and J. Lilie, *J. Phys. Chem.*, 1981, **85**, 1246.
65 A. Henglein, M. Gutierrez, E. Janata and B. G. Ershov, *J. Phys. Chem.*, 1992, **96**, 4598.
66 J. Westerhausen, A. Henglein and J. Lilie, *Ber. Bunsenges. Phys. Chem.*, 1981, **85**, 182.
67 S. Mosseri, A. Henglein and E. Janata, *J. Phys. Chem.*, 1989, **93**, 6791.
68 B. Cercek, M. Ebert and A. J. Swallow *J. Chem. Soc. A*, 1966, 612.
69 J. Butler and A. Henglein, *Radiat. Phys. Chem.*, 1980, **15**, 603.
70 G. V. Buxton, T. Rhodes and R. Sellers, *J. Chem. Soc., Faraday Trans. 1*, 1982, **78**, 3341.
71 M. Breitenkamp, A. Henglein and J. Lilie, *Ber. Bunsenges. Phys. Chem.*, 1976, **80**, 973.
72 A. Henglein, E. Janata and A. Fojtik, *J. Phys. Chem.*, 1992, **96**, 4734.
73 M. Gutierrez and A. Henglein., *J. Phys. Chem.*, 1996, **100**, 7656.
74 B. Keita, L. Nadjo, E. Gachard, H. Remita, J. Khatouri and J. Belloni, *New J. Chem.*, 1997, **21**, 851.
75 A. Henglein and M. Giersig, *J. Phys. Chem.*, 1994, **98**, 6931.
76 J. Khatouri, M. Mostafavi, J. Amblard and J. Belloni, *Z. Phys. D*, 1993, **26**, 82.
77 J. Belloni, in *Homogeneous Photocatalysis*, ed. M. Chanon, John Wiley, Chichester, 1997, vol. 2, pp.169–218.
78 C. de Cointet, M. Mostafavi, J. Khatouri and J. Belloni, *J. Phys. Chem.*, 1997, **18**, 3512.
79 C. de Cointet, J. Khatouri, M. Mostafavi and J. Belloni, *J. Phys. Chem.*, 1997, **18**, 3517.
80 E. Gachard, H. Remita, J. Khatouri, J. Belloni, B. Keita and L. Nadjo, following paper.
81 J. Belloni, M. O. Delcourt and C. Leclere, *Nouv. J. Chim.*, 1982, **6**, 507.
82 J. Belloni and M. Lecheheb, *Radiat. Phys. Chem.*, 1987, **29**, 89.
83 N. Keghouche, Thesis, University of Constantine, 1993.
84 B. Le Gratiet, Thesis, Université de Paris-Sud, Orsay, 1996.
85 J. Bruneaux, H. Cachet, M. Froment, J. Amblard, J. Belloni and M. Mostafavi, *Electrochim. Acta*, 1987, **32**, 1533.
86 J. Bruneaux, H. Cachet, M. Froment, J. Amblard and M. Mostafavi, *J. Electroanal. Chem.*, 1989, **269**, 375.
87 T. Gacoin, F. Chaput, J. P. Boilot, M. Mostafavi and M. O. Delcourt, in *Eurogel 91 Progress and Development of Processes and Products from Sols and Gels*, ed. S. Vilminot, R. Nass and H. Schmidt, E-MRS, North Holland, Amsterdam, 1991, pp. 159–166.
88 D. Lawless, S. Kapoor, P. Kennepohl, D. Meisel and N. Serpone, *J. Phys. Chem.*, 1994, **98**, 9616.
89 J. Amblard, O. Platzer, J. Ridard and J. Belloni, *J. Phys. Chem.*, 1992, **96**, 2340.
90 J. Michalik, N. Azuma, J. Sadlo and L. Kevan, *J. Phys. Chem.*, 1995, **99**, 4679.
91 E. Gachard, J. Belloni and M. A. Subramanian, *J. Mater. Chem.*, 1996, **6**, 867.
92 A. Malkov and J. Belloni, *J. Chim. Phys.*, 1992, **89**, 885.
93 B. G. Ershov, E. Janata and A. Henglein, *J. Phys. Chem.*, 1994, **98**, 7619.
94 B. G. Ershov, E. Janata and A. Henglein, *J. Phys. Chem.*, 1994, **98**, 10891; *Radiat. Phys. Chem.*, 1996, **47**, 59.
95 J. Belloni, M. O. Delcourt, J. L. Marignier and J. Amblard, in *Radiation Chemistry*, ed. P. Hedwig, L. Nyikos and R. Schiller, Akad. Kiado, Budapest, 1987, pp. 89–95.
96 M. Treguer, C. de Cointet, H. Remita, J. Khatouri, M. Mostafavi, J. Amblard, J. Belloni and R. de Keyzer, *J. Phys. Chem.*, 1998, **102**, 4310.
97 Agfa GV *Eur. Pat.* 95203 1706, 1995.
98 S. Remita, G. Picq, J. Khatouri and M. Mostafavi, unpublished work.
99 A. Henglein and R. Tausch-Treml, *J. Colloid Interface Sci.*, 1981, **80**, 84.
100 J. Khatouri, M. Mostafavi, J. Amblard and J. Belloni, *Z. Phys. D, Atoms, Molecules, Clusters*, 1993, **26**, 82.
101 T. Sosebee, M. Giersig, A. Holzwarth and P. Mulvaney, *Ber. Bunsenges. Phys. Chem.*, 1995, **99**, 40.
102 M. Mostafavi, unpublished results.
103 S. Remita, M. Mostafavi and M. O. Delcourt, *Radiat. Phys. Chem.*, 1996, **47**, 275.
104 P. Mulvaney, *Langmuir*, 1996, **12**, 788.
105 H. Remita, J. Khatouri, M. Treguer, J. Amblard and J. Belloni, *Z. Phys. D, Atoms, Molecules, Clusters*, 1997, **40**, 127.
106 J. Amblard, O. Platzer and J. Belloni, *J. Chim. Phys.*, 1991, **88**, 835.
107 J. Belloni, J. Khatouri, M. Mostafavi and J. Amblard, in *Imaging on the Information Superhighway*, ed. M. Sahyun, IST, Town?, 1995, pp. 315–318.
108 J. L. Marignier, M. Ashokkumar and M. Mostafavi, in *A celebration of all Imaging*, IST, Town?, 1997, pp. 67–71.
109 Agfa GV, *Eur. Pat.* 774960, 1995.
110 B. Le Gratiet, H. Remita, G. Picq and M. O. Delcourt, unpublished work.

Received in Montpellier, France, 19th February 1998*;*
Paper 8/01445K